1-1-2017

Small Rho GTPase Family Member Cdc42 and Its Role in Neuronal Survival and Apoptosis

Noelle Christine Punessen
University of Denver

Small Rho GTPase Family Member Cdc42 and Its Role in Neuronal Survival and Apoptosis

Abstract

Neurodegenerative diseases such as amyotrophic lateral sclerosis (ALS), Alzheimer's and Parkinson's disease are caused by a progressive and aberrant destruction of neurons in the brain and spinal cord. These disorders lack effective long term treatments, and existing options focus primarily on either delaying disease onset or alleviating symptomology. Dysregulated programmed cell death, known as apoptosis, is one of the most significant contributors to neurodegeneration, and is controlled by a number of different factors. Rho GTPases are a protein class with recognized importance in proper neuronal development and migration, and have more recently emerged as regulators of apoptosis and neuronal survival. Here, we investigated the role of Rho GTPase family member Cdc42 and its downstream effectors in neuronal survival and apoptosis. Our goal was to determine whether a Cdc42 signaling pathway contributes to the survival of neurons subjected to arduous growth conditions, simulating pathophysiological stress endured during neurodegeneration. We initially induced apoptosis in rat cerebellar granule neurons (CGNs) by removing both growth factor-containing serum and depolarizing potassium from the cell media. We then utilized both chemical inhibitors and adenoviral Cdc42 shRNA to block the function of Cdc42 or its downstream effectors in this stressful growth environment. Our *in vitro* studies demonstrate that functional inhibition of Cdc42 or two of its downstream targets (ACK-1 and PAK) did significantly sensitize neurons to cell death under duress. Our results advocate a pro-survival role for Cdc42 in neurons, and propose that it could be a potential therapeutic target for decelerating the advancement of neurodegenerative disease.

Document Type
Thesis

Degree Name
M.S.

Department
Biological Sciences

First Advisor
Daniel A. Linseman, Ph.D.

Second Advisor
Todd Blankenship

Third Advisor
Michelle Knowles

Keywords
Cdc42, Cell division control protein 42, Amyotrophic Lateral Sclerosis, ALS, Rho GTPase, Neurodegenerative disease, Therapies

Subject Categories
Biology | Genetics and Genomics

Publication Statement

Copyright is held by the author. User is responsible for all copyright compliance.

Small Rho GTPase Family Member Cdc42 and its Role in Neuronal Survival and

Apoptosis

_____

A Thesis

Presented to

the Faculty of Natural Sciences and Mathematics

University of Denver

_____

In Partial Fulfillment

of the Requirements for the Degree

Master of Science

_____

by

Noelle C. Punessen

August 2017

Advisor: Dr. Daniel A. Linseman

Abstract

Neurodegenerative diseases such as amyotrophic lateral sclerosis (ALS),

Alzheimer's and Parkinson's disease are caused by a progressive and aberrant destruction

of neurons in the brain and spinal cord. These disorders lack effective long term

treatments, and existing options focus primarily on either delaying disease onset or

alleviating symptomology. Dysregulated programmed cell death, known as apoptosis, is

one of the most significant contributors to neurodegeneration, and is controlled by a

number of different factors. Rho GTPases are a protein class with recognized importance

in proper neuronal development and migration, and have more recently emerged as

regulators of apoptosis and neuronal survival. Here, we investigated the role of Rho

GTPase family member Cdc42 and its downstream effectors in neuronal survival and

apoptosis. Our goal was to determine whether a Cdc42 signaling pathway contributes to

the survival of neurons subjected to arduous growth conditions, simulating

pathophysiological stress endured during neurodegeneration. We initially induced

apoptosis in rat cerebellar granule neurons (CGNs) by removing both growth factor-

containing serum and depolarizing potassium from the cell media. We then utilized both

chemical inhibitors and adenoviral Cdc42 shRNA to block the function of Cdc42 or its

downstream effectors in this stressful growth environment. Our *in vitro* studies

demonstrate that functional inhibition of Cdc42 or two of its downstream targets (ACK-1

and PAK) did significantly sensitize neurons to cell death under duress. Our results

advocate a pro-survival role for Cdc42 in neurons, and propose that it could be a potential

therapeutic target for decelerating the advancement of neurodegenerative disease.

iv

Table of Contents

List of Figures

Chapter One: Introduction

1.1 Neurodegenerative Disease and Cell Death

Cell death is a natural and necessary event in the life cycle of a cell that ensures

proper development and maintains organismal homeostasis. During development of the

nervous system, approximately half of all newly formed neurons will die by the early

postnatal period in order to ensure proper neural connection formation and function

(Oppenheim, 1991). Cell death can transpire through various distinct mechanisms, and it

is a requirement of normal cells in order to replace aged or damaged cells with healthy,

optimally functional ones. These death mechanisms can be the result of pre-programmed

instructions as a response to intracellular signaling (i.e., apoptosis, autophagy,

necroptosis, anoikis), or a consequence of cellular infection or injury (i.e., necrosis,

oncosis, mitotic catastrophe) (Duprez et al. 2009, Krysko et al. 2009, Vakifahmetoglu et

al. 2008). While cell death is considered an essential phase in the cellular life cycle, it

must also be a tightly controlled process, as its dysregulation has several pathological

repercussions.

Neurodegeneration is described as the loss of structure and/or function in nerve

cells, eventually leading to neuronal death. In neurodegenerative disease, cell death

mechanisms are hyperactivated due to pathophysiological culprits such as oxidative

stress, mitochondrial dysfunction or excitotoxicity (Martin et al. 1998, Beal, M.F. 1998,

Chen et al. 2012), and neurons in the brain and spinal cord are subsequently aberrantly

and prematurely destroyed. Because neurons cannot divide and reproduce, they cannot replenish themselves once they are lost. The progressive loss of neuronal populations in diseases such as Alzheimer's, Parkinson's and amyotrophic lateral sclerosis (ALS) then leads to deterioration of cognitive and motor function in those afflicted. Additionally, treatments for these disorders are limited both in number and in efficacy, typically aiming to alleviate symptoms or delay disease onset or progression. The current economic cost associated with health care of these patients and their families is well within the billions, and due to the obscure pathogenesis of neurodegenerative diseases, it is not likely to decrease anytime soon (Brown et al. 2005). The detrimental and incurable nature of neurodegenerative disease has guided research to focus either on more accurately delineating causative factors in these disorders, or in identifying therapeutic agents or targets that could improve patient quality of life.

1.2 Cancer and Cell Survival

Opposite to neurodegeneration on the disease spectrum is cancer. Prior to the demise of a cell, it must respond to survival promoting biological signals, which are also highly regulated in order to keep it healthy and functional. Bcl-2 anti-apoptotic protein family members (i.e., Bcl-2, Bcl-XL), growth factors, inhibitor of apoptosis proteins (IAPs), and other mitogenic proteins that activate pro-survival pathways (i.e., PI3K/Akt, MEK/ERK) are some examples of key players in the cell survival signaling (Portt et al. 2011). Like cell death, there are also pathological consequences if survival is not controlled appropriately.

Cancer is often viewed as a profusion of uncontrolled cell growth and atypical cell migration. It can further be described as a summative consequence of cell cycle malfunctions that allow abnormal cells to progress through the cell cycle instead of being destroyed, causing a build-up of mutations and abnormal cell proliferation (Foster, 2006). Mutations in healthy cells can be the result of a genetic predisposition, exposure to carcinogenic materials, or otherwise DNA-damaging factors. Cancerous cells are able to evolve in a way that prevents their destruction, and they possess several unique characteristics that normal cells do not, including adhesion-independent growth ability, unscheduled proliferation, insensitivity to apoptotic signals and metastatic capability. These erratic transformations make it exceedingly difficult to isolate therapeutic targets in cancer treatment.

The prevalence of cancer in the U.S., as well as in most other countries, is on the rise due to unhealthy lifestyle choices, environmental changes (i.e., pollution, ozone depletion) and an increase in the elderly population as a whole. Also, screening and diagnosis techniques for cancer are much improved. Consequently, both cancer research and treatment have become substantial economic financial burdens, and much of current cancer research focuses on prevention and improvement of existing treatment options (i.e., chemotherapy, radiation, etc.) (Yabroff et al. 2011). Because cellular and organismal homeostasis depend on the delicate balance between cell survival and death, it is not surprising that both pathways share many common signaling components.

1.3 Introduction to Rho Family GTPases: Structure, Function and Regulation

The Rho GTPase subfamily is a class of proteins belonging to the Ras superfamily of low molecular weight (~21 kDa) guanosine triphosphatases. While they are best known for their role in regulation of actin cytoskeletal dynamics, these monomeric proteins have also been implicated in many other functional areas, such as the regulation of various transcription factors (Hall, 2005), development and maintenance of cell polarity (Nobes et al. 1999) and cell cycle progression (Olson et al. 1995). Rho GTPases can be activated by many extracellular signals, including growth factor receptors, receptor tyrosine kinases, cytokine receptors, G-protein coupled receptors (GPCRs) and integrins (Sinha and Yang, 2008). Once activated, they signal downstream to various effectors to promote biological responses.

All Rho GTPases contain a common G-domain region, which mediates the binding of guanine nucleotides, as well as a Rho insert region that mediates isoform specific effector binding, and a hypervariable C-terminal region that assists in membrane binding (Schaefer et al. 2014). The cyclic activation of Rho GTPases relies on their guanine nucleotide binding status, becoming active when GTP bound and inactive when GDP bound (Figure 1). Rho GTPases are often referred to as molecular "switches", due to conformational changes that arise when they are activated. These conformational changes take place mainly in two notable regions, referred to as switch I and switch II, wherein the γ-phosphate of GTP will bind and relay activation information. Once GTP hydrolysis occurs, and the γ-phosphate is lost, the switch regions will relax again (Schaefer et al. 2014). While the guanine nucleotide binding domain of Rho GTPases is

important for determination of switch region conformation, and subsequent effector activation, Mg^{2+} binding is also imperative in controlling the initial affinity of the GTPase for nucleotide binding (Rossman et al. 2005).

There are three general classes of proteins that regulate Rho GTPase activation, including guanine nucleotide exchange factors (GEFs), GTPase activating proteins (GAPs) and guanine nucleotide dissociation inhibitors (GDIs). GEFs are the activating proteins of GTPases that facilitate the exchange of GDP for GTP, while GAPs promote GTPase inactivation by stimulating their intrinsic ability to hydrolyze GTP to GDP. GDIs are responsible for the sequestration of inactive (GDP-bound) GTPases in the cytosol, and it is their dissociation that controls membrane localization and subsequent activation of the Rho GTPase family (Hakoshima et al. 2003). Rho GTPase activity is also regulated by other factors, such as membrane localization and specificity of GEF/GAP or effector interactions. There are currently over 70 GEFs, 60 GAPs and 3 GDIs known to interact with Rho GTPases (Valdés-Mora et al. 2009).
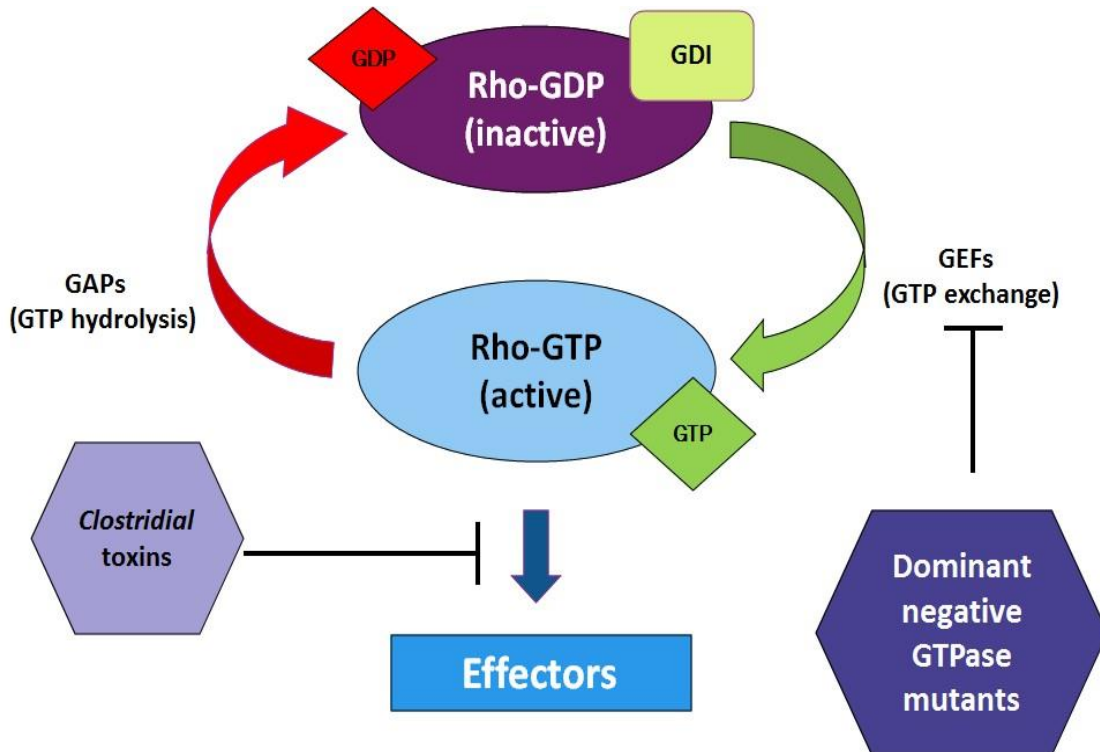
Figure 1: Cyclic activation/inactivation of Rho family GTPases. Rho family GTPases cycle between an inactive (GDP-bound) state and an active (GTP-bound) state. This is facilitated by activators known as guanine nucleotide exchange factors (GEFs) that catalyze the exchange of GDP for GTP, and inactivators known as GTPase activating proteins (GAPs) that stimulate the intrinsic ability of GTPases to hydrolyze GTP to GDP. Additionally, guanine nucleotide dissociation inhibitors (GDIs) sequester GTPases in an inactive state in the cytosol to regulate their activity. Both *Clostridial* toxins and dominant negative GTPase mutants have been used in prior experiments to block the activity of Rho GTPases in order to delineate their biological functions.

1.3.1 The Role of Rho GTPases in Regulating Actin Cytoskeletal Dynamics

Rho GTPases are well known for their role in regulating dendritic spine morphogenesis, growth cone motility and axonal migration (Linseman and Loucks, 2007). Although there are seven subfamilies of Rho GTPase members (Rho, Rac, Cdc42, Rnd, RhoD, RhoBTB, RhoH), the most extensively studied members to date are RhoA, Rac1 and Cdc42. Previous fibroblast based research has demonstrated that specifically, RhoA promotes development of actin stress fibers, Rac1 propagates lamellipodia and membrane ruffle development, and Cdc42 mainly contributes to the development of actin microspikes and filopodia (Govek et al. 2005). It is also understood that these Rho GTPase family members tend to antagonize each other in cytoskeletal regulation. Rac1 tends to promote growth cone development and neuronal branching, as demonstrated in dominant negative *Caenorhabditis elegans* Rac1 mutants that display neuronal branching defects (Lundquist, 2003). Cdc42 stimulates growth cone rearrangement and axonal guidance, as seen in studies of dominant negative Cdc42 mutants expressed in chick retinal ganglion cells that were defective in those abilities (Rosdahl et al. 2003). Alternatively, RhoA has been found to induce neurite retraction and growth cone collapse, as seen in studies of a mouse neuroblastoma cell line (N1E-115) where RhoA was activated using the GPCR agonist lysophosphatidic acid (LPA) (Kranenburg et al. 1999). A delicate balance between the function of each GTPase must be maintained for proper neuronal development and plasticity.

Although Rac generally plays a growth promoting role and Rho antagonizes this in most cell lines, a few notable exceptions have been discovered. In sympathetic, dorsal

root ganglion (DRG) cells, a dominant negative mutant Rac1 caused neurite extension (Fournier et al. 2003), while constitutively active Rac1 mutant expression enhanced DRG growth cone collapse and a decrease in neurite length in mouse cortical neurons (Jin and Strittmatter, 1997, Vastrik et al. 1999, Kubo et al. 2002). Similarly, another study found that in mouse hippocampal neuron cultures, dominant negative RhoA expression inhibited axonal growth (Ahnert-Hilger et al. 2004). These examples of differences observed in GTPase function might be due to discrepancies between cell and organism type, or in experimental approaches.

1.3.2 The Role of Rho GTPases in Neuronal Survival and Apoptosis

Due to their intimate relationship with actin cytoskeletal regulation, it is not surprising that roles in neuronal survival and death have emerged for Rho GTPase family members. Neurite initiation, axonal guidance and growth, neuronal migration, dendritic morphology, and synapse formation all rely on Rho GTPase activity (Luo, 2000, Govek et al. 2005). More recently, a role in neuronal survival has also been ascribed to two of the three well-known Rho family members. It has been reported that Rac1 and RhoA functionally antagonize each other in a survival context, where Rac1 primarily plays a pro-survival role and causes neurite extension, while RhoA displays pro-apoptotic qualities, and induces neurite retraction (Linseman and Loucks, 2007, Govek et al. 2005, Stankiewicz and Linseman, 2014). Studies in primary cortical neurons have also demonstrated the importance of Rho GTPases in neuronal survival, as statin inhibitors

were shown to decrease GTPase membrane association through a reduction in mevalonate synthesis, and thus induce apoptosis (Chuang et al. 1997).

The pro-survival characteristics of Rac1 have been in part attributed to signaling its downstream effector p21-activated kinase (PAK), which promotes survival through activation of a mitogen activated protein kinase (MAPK) MEK1/2/ERK1/2 pathway. This pathway induces degradation of pro-apoptotic BH3-only family member Bim, and suppresses pro-apoptotic JAK/STAT signaling (Loucks et al. 2006). Stankiewicz et al. (2012) also demonstrated that CGN apoptosis following exposure to *Clostridial* Toxin B is also due to a JAK/STAT5 pathway specifically. Finally, Rac1 also phosphorylates phosphoinositide-3-kinase (PI3K), which stimulates cell survival via Akt phosphorylation of pro-apoptotic protein Bad (Datta et al. 1997). Alternatively, RhoA propagates neuronal death by activating its major downstream pathway, Rho-associated protein kinase/phosphatase and tensin homolog (ROCK/PTEN), which dephosphorylates phosphatidylinositol (3,4,5)-trisphosphate (PIP_3) to phosphatidylinositol 4,5-bisphosphate (PIP_2) to terminate Rac activation of Akt (Lai et al. 2014). Although these oppositional roles have been elucidated for several neuronal cell types, there are also exceptions to the generally accepted notion that Rac is pro-survival and Rho is pro-apoptotic. For example, deletion of Rac1/Cdc42 function in sympathetic neurons has been shown to inhibit a cJun/JNK-dependent apoptotic pathway, and to protect them from apoptosis caused by removal of nerve growth factor (Linseman et al. 2001), which is an *in vitro* survival requirement of for them.

Although a role in neuronal survival and apoptosis has been described for both RhoA and Rac1, the role of Cdc42 has not been as clearly defined. Le et al. (2005) have previously proven that inhibition of Rac function with either dominant negative mutants or *Clostridial* toxin B (a broad Rho GTPase family inhibitor) will induce neuronal death, but a dominant negative Cdc42 did not cause the same induction of apoptosis. This suggests that Rac is the main Rho GTPase contributor in neuronal survival. Cdc42 function has consistently demonstrated promotion of cellular growth and survival in a number of other cell types, so it is not unlikely that it plays a part in neuronal survival as well. Additionally, cross-talk between Rho GTPase family members, sequence homology between Rac and Cdc42 (~70%) (Hakoshima et al. 2003), and pathologically related findings of Rho family members and/or their effectors all advocate a possible role for Cdc42 in neuronal survival.

Understanding of the role Rho GTPases play in neuronal survival and development has led to the discovery of dysfunctional Rho GTPase signaling in various nervous system disorders. Diminished Rac1 activity and/or hyperactive RhoA signaling have been implicated in neurodegenerative diseases such as Huntington's, Alzheimer's and Parkinson's disease (Stankiewicz and Linseman, 2014). Deregulated Rho GTPase signaling components aside from the GTPase itself have also been pathologically linked. For example, mutations in a Rac specific GEF known as alsin have been causally connected to the development of juvenile onset ALS (Hadano et al. 2007). Additionally, Rac and Rho have also been implicated in regulating cellular survival and recovery after nervous system damage. For example, decreased Rho signaling and increased Rac

signaling have demonstrated importance in axonal regeneration following spinal cord injury, as well as prevention of neuronal death after ischemic injuries such as stroke (Stankiewicz and Linseman, 2014). Cdc42 and its many effectors have also been pathologically implicated in neurodegenerative disease. For example, genetic mutations in mental X-linked retardation (MRX) have been found to induce malfunctions in a protein that serves as a Cdc42 GAP (i.e., Oligophrenin-1), as well as in downstream Cdc42 effector protein, PAK (Schmidt and Hall, 2002). Defective Cdc42 signaling has also been linked to ailments of other bodily systems such as immune disorders (i.e., Wiskott-Aldrich syndrome), faciogenital dysplasia and cardiovascular disorders (Tu and Cerione, 2001, Schmidt and Hall, 2002).

1.4 Cell Division Control Protein 42 (Cdc42)

Cell division control protein 42 (Cdc42) was originally studied in *Saccharomyces cerevisiae* (yeast) as a regulator of polarity and bud growth (Zheng et al. 1996). It is a ~21 kDa, ubiquitously expressed protein with homologs in several species, and has two known alternatively spliced isoforms, including placental Cdc42 and a brain isoform (Shinjo et al. 1990). The human homolog (often referred to as G25K) shares approximately 50% sequence homology with mammalian Rho and 70% with Rac (Munemitsu et al. 1990). Cdc42 is localized to many intracellular membranes, including the plasma membrane, Golgi apparatus and vesicular membranes (Shinjo et al. 1990). It interacts with cellular membranes via post-translational geranylgeranylation of its C-

terminus, or it can exist freely in the cytosol when its geranylgeranyl moiety is bound to a GDI (Resh, 2013).

Cdc42 has two known families of GEFs: the Diffuse B-cell lymphoma (Dbl) family, which contain conserved Dbl homology (DH)/Pleckstrin homology (PH) domains in tandem, and the Dedicator of Cytokinesis (DOCK) atypical family, which lacks the aforementioned DH domain and instead contain Dock180 homology domains DHR1 and DHR2 (Sinha and Yang, 2008). The DH domain of Dbl family GEFs directly binds Cdc42 to cause GDP dissociation and GTP exchange, and thus is critical for GEF activity. The PH domain of these GEFs is equally important for GEF activity, and is responsible for binding Cdc42 target proteins, phosphoinositide interaction and membrane targeting (Sinha and Yang, 2008). DOCK GEFs specific to Cdc42 include Zizimin1 (DOCK9) and ACG (Zizimin2/DOCK11) (Meller et al. 2005). While the PH domain in DOCK GEFs has a function analogous to that in Dbl GEfs, it is the DHR2 domain in these GEFs that catalyzes the GDP-GTP exchange (Côté and Vuori, 2006).

Cdc42 is a homodimer which, in addition to the structural elements of GTPases described earlier, also sequentially includes a GTP-binding protein domain and a phosphate-binding loop (P-loop) containing nucleoside triphosphate hydrolase, which functions in its intrinsic GTP hydrolysis activity (Protein Data Bank in Europe). It transduces information from various different extracellular signals, including cytokines, growth factors, GPCR ligands, proteoglycans and integrins in order to exert a number of physiological effects (Symons and Settleman, 2000). The most well characterized duty of Cdc42 is its actin polymerizing role critical to the formation of filopodia, which extend

12

from the leading edges of cells to environmental probing and the formation cell-cell contacts (Gupton and Gertler, 2007). Other functions of Cdc42 include G1/S phase progression in the cell cycle and mitotic development (Stengel and Zheng, 2011), regulation of cell polarity, cellular migration and chemotaxis, cell fate determination, transcriptional control and intracellular trafficking (Valdés-Mora et al. 2009). Most of what is known about Cdc42 in relation to mammalian physiology comes from dominant negative or constitutively active mutational studies, though more recent genetic studies in mice have provided insight into other cell-type and tissue-type biological functions of Cdc42 (Melendez et al. 2011).

1.4.1 Cdc42 in Pathology

One research area of great current interest is the involvement of Cdc42 in cancer. Because it has well-described roles in cellular migration, filopodia development, and cell cycle regulation, it is not surprising that Cdc42 and its downstream targets have been consistently linked to tumorigenesis, cancer progression and metastasis. Increased levels of Cdc42 expression have been reported in a diversity of cancer types, including colorectal adenocarcinoma, non-small cell lung carcinoma, melanoma, breast and testicular cancer. Furthermore, increased activity of Cdc42 downstream target ACK-1 has also been implicated in the progression of both prostate and breast cancer (Mahajan and Mahajan, 2010). Although no mutations in the human *Cdc42* gene itself have been detected thus far in cancer, it is the overexpression of the Cdc42 protein, or aberrant

downstream pathway signaling that appear to be correlated with both poor patient prognosis and increased metastatic potential (Stengel and Zheng, 2011).

The oncogenic potential of Cdc42 has been extensively defined, and its contribution to cellular transformation includes interplay with Ras (Qiu et al. 1997), prevention of appropriate epidermal growth factor receptor (EGFR) degradation (Wu et al. 2003), and cooperation with dysfunctional activity in tumor suppressors such as p53 and p19ARF to promote tumor growth (Guo and Zheng, 2004). A study performed by Lin et al. (1997) described how mutational disruption of the Cdc42 activation cycle, wherein it was able to spontaneously bind GTP while GTP hydrolysis rates remained static, caused reduced dependency on culture serum and anchorage-independent growth capability in a fibroblast cell line. Another study by Ye et al. (2015) detailed how increased Cdc42 protein levels contributed to the migration of HeLa cervical cancer cells, likely through enhanced filopodia formation. Additionally, Cdc42 has exhibited ability to positively regulate transcription at survival and proliferation stimulating NF□B promoters, which allows deleteriously transformed cells to escape apoptotic destruction (Boettner and Van Aelst, 2002). Interestingly, in few instances, Cdc42 has also been reported to exert inhibitory effects on cell growth (Valdés-Mora et al. 2009). For example, a functional knockout study done by Vega and Ridley (2008) of Cdc42 in liver cells actually caused an increase in liver cancer progression, and Cdc42 knockout in Jurkat T lymphocytes has been found to cause JNK pathway-dependent caspase activation and apoptosis (Chuang et al. 1997), which would indicate a lack of pro-survival acivity in these circumstances. Although exceptions exist, they appear to be

tissue type and cell type specific, and Cdc42 is generally recognized as a growth promotional protein.

Although cancer consumes the largest investigational area in Cdc42-linked disease research, it is not alone. As mentioned previously, dysregulation of Cdc42 and its interacting proteins has been connected to a wide range of disorders, such as faciogenital dysplasia (Zheng et al. 1996), Fanconi anemia (Zhang et al. 2008), Huntington's disease (Holbert et al. 2003) and immune disorder Wiskott-Aldrich syndrome (Kirchhausen and Rosen, 1996). Downstream signaling pathways involved in some of these disorders will be more thoroughly discussed later.

1.5 Downstream Effectors of Cdc42

There are many known target proteins of Cdc42, but for our study we chose to focus on three: activated cdc42 kinase-1 (ACK-1), p21 activated kinase (PAK) and neuronal Wiskott-Aldrich syndrome protein (N-WASp). Each of these effector proteins chosen contains a highly conserved Cdc42/Rac-interactive binding (CRIB) motif within their GTPase binding domain (GBD) (Burbelo et al. 1995). As the name would suggest, this domain dictates effector binding to Cdc42. It was discovered using nuclear magnetic resonance (NMR) studies of active Cdc42 bound to downstream effectors containing the motif, and is cited as necessary, but not sufficient for tight Cdc42 binding (Hoffman and Cerione, 2000). Because these three downstream target proteins share a common GTPase CRIB binding domain and have similar Cdc42 binding affinity, determination of which

Cdc42-effector pathway is triggered upon Cdc42 activation is believed to be guided by which specific upstream signal and/or GEF interacts with Cdc42 (Sinha and Yang, 2008).

1.5.1 Activated Cdc42 Kinase-1 (ACK-1)

Activated Cdc42 kinase 1 (ACK-1) is a ~120 kDa non-receptor tyrosine kinase that is a downstream effector specific to Cdc42. There are two isoforms (ACK-1 and ACK-2), both of which are expressed throughout the body, but are especially enriched in the brain (Hoffman and Cerione, 2000). Its structure consists of an amino-terminal sterile α motif (SAM) domain responsible for membrane targeting, an N-terminal tyrosine kinase domain, an EGFR binding domain (EBD) and a C terminus containing both a GBD with a CRIB motif, as well as a ubiquitination (UBA) domain involved in ACK-1 protein turnover (Lougheed et al. 2004, Mahajan and Mahajan, 2010). The exact mechanism of ACK-1 activation is still relatively unclear, although most report it to exist in an autoinhibitory state (Figure 2A), wherein interaction between the EBD and kinase domain prevents its kinase activity (Mahajan and Mahajan, 2015) until GTPase binding or activation by ligand binding of tyrosine kinase receptors (Figure 2B).
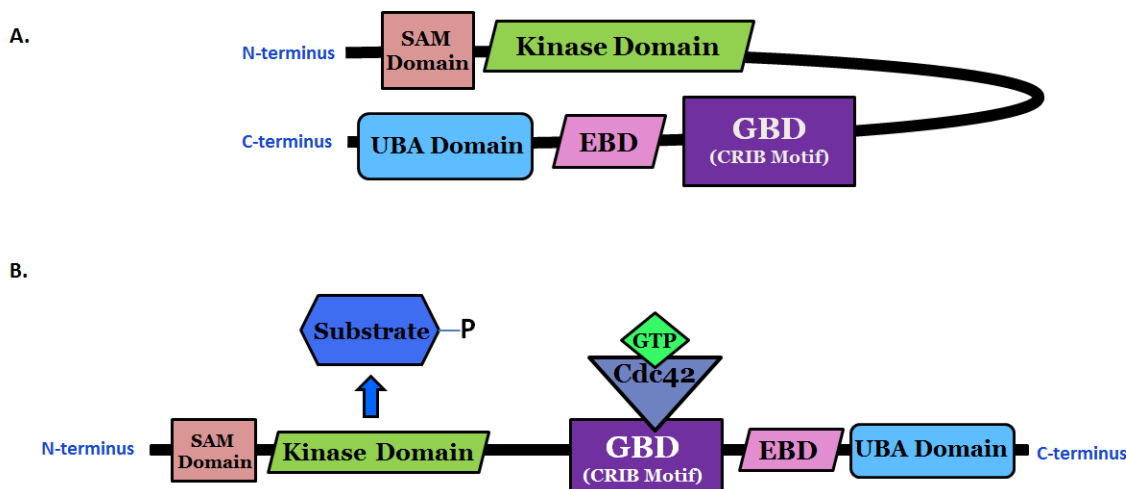
Figure 2: Inactive and active conformations of Cdc42 effector ACK-1. A. Schematic representation of autoinhibited ACK-1. Interaction between the EGFR binding domain (EBD) and N-terminal kinase domain prevent its function. **B.** Functionally active, GTP-Cdc42 bound conformation of ACK-1. Cdc42 binding to the GBD releases the kinase domain, so that ACK-1 may phosphorylate its substrates.

Upon Cdc42 activation, ACK-1 stimulates a plethora of signaling cascades (Figure 3), such as the PI3K/Akt pathway and the androgen receptor (AR) to incite the survival and proliferation of cells (Mahajan and Mahajan, 2010). It is also involved in regulation of actin cytoskeletal arrangement and cell migration via signaling proteins such as the p130^{Cas} adaptor molecule, a critical component of integrin-mediated cell motility, and formation of a complex with p130^{Cas} and Crk proteins (Modzelewska et al. 2006). Additionally, ACK-1 has demonstrated ability to phosphorylate and activate Wiskott-Aldrich syndrome protein (WASp) in order to regulate actin dynamics (Yokoyama et al. 2005). In a neuronal context, Linseman et al. (2008) described how ACK-1 contributes to neurite outgrowth after muscarinic cholinergic receptor (mAChR) activation in a human neuroblastoma cell line, attributable to ACK-1 phosphorylation by Fyn kinase downstream of Rho kinase signals. Finally, ACK-1 has demonstrated anti-

apoptotic qualities in the *Drosophila* eye*,* wherein it interacts with a Grb2 homolog and a transcriptional co-activator to promote proliferative and anti-apoptotic gene transcription (Schoenherr et al. 2012).

ACK-1 is pathologically relevant, and elevated levels of the ACK-1 gene in tumors has been positively correlated with poor prognosis and increased cancer cell invasiveness (Schoenherr et al. 2012). Increased levels of ACK-1 mRNA have also been identified in various cancer types, including cervical, breast, prostate, ovarian, lung, gastric, and cancers of the head and neck (Mahajan and Mahajan, 2010, Mahajan et al. 2007, Mahajan and Mahajan, 2015). The contribution of ACK-1 to cancer progression stems from its ability to upregulate both AR and Akt, and simultaneously cause the phosphorylation and degradation of tumor suppressor WW domain-containing oxioreductase (Wwox) (Mahajan and Mahajan, 2010) (Figure 3). Mahajan et al. (2005) have described *in vivo* studies of nude mice wherein ACK-1 upregulation was found to assist in the development of anchorage-independent growth and tumorigenesis.

ACK-1 signaling is also crucial in central nervous system development, and has shown elevated levels in the cerebellum, hippocampus and neocortex (Ureña et al. 2005), with even greater increases in areas of proliferation and migration during development in the rat brain (La Torre et al. 2006). In terms of neural disorders, ACK-1 has been implicated in infantile onset epilepsy, due to a genetic mutation that upregulated protein levels (Ureña et al. 2005), as well as autism spectrum disorder and attention deficit/hyperactivity disorder through its effects on dopamine transporter plasma membrane stabilization (Wu et al. 2015). We chose to focus mainly on ACK-1 out of the

three effectors investigated, as it is targeted only by Cdc42 GTPase and has explicitly

demonstrated importance in cellular survival in previous studies.
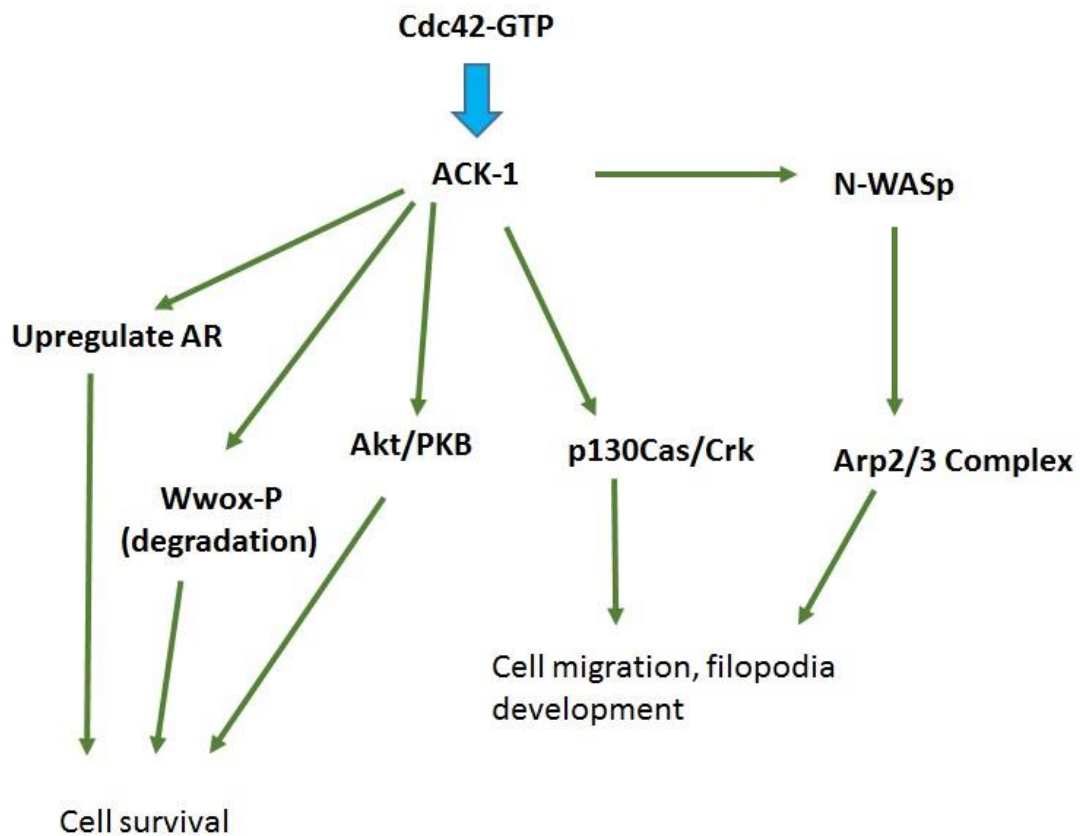
Figure 3. ACK-1 signaling pathways involved in actin cytoskeletal regulation and cell survival. ACK-1 activation by GTP-Cdc42 has several actin regulatory and cell migratory effects, including aiding in the development of filopodia. This occurs both through ACK-1 phosphorylation of neuronal Wiskott-Aldrich syndrome protein (N-WASp), as well as ACK-1 phosphorylation of docking protein p130^{Cas}, which forms a complex with adaptor protein Crk that is critical in integrin-mediated cell migration. ACK-1 activation also supports cellular survival through activation of the pro-survival PI3K/Akt pathway, which negatively regulates pro-apoptotic Bcl-2 family members, phosphorylation/degradation of the tumor suppressor protein Wwox, and upregulation of androgen receptors.

1.5.2 p21 Activated Kinase (PAK)

p-21 activated kinase (PAK) proteins are a serine/threonine kinase family targeted by both Cdc42 and Rac (Hanna and El-Sibai, 2013). There are six known PAK isoforms, organized into Group I (PAKs 1-3) and Group II (PAKs 4-6) (Itakura et al. 2013), although PAK1, PAK2 and PAK3 are the most well characterized and have explicitly demonstrated kinase activity upon Rac/Cdc42 interaction (Wells and Jones, 2010). Figure 4A shows the structure of PAK proteins, with a regulatory N-terminal domain containing the GBD and the CRIB motif that is overlapped by an autoinhibitory domain (AID) (Dummler et al. 2009). Once Cdc42 binds and activates PAK, it results in its autophosphorylation, and subsequent disruption of the autoinhibitory relationship between the N-terminus and the catalytic C-terminal kinase domain (Figure 4B) (Lei et al. 2000, Buchwald et al. 2001). There are various GTPase-independent activating mechanisms for PAK proteins, including cyclin-dependent kinase 5, adaptor proteins Nck and Grb2, and sphingolipids (Dummler et al. 2009), but these will not be discussed here. Once activated, PAK proteins then proceed to phosphorylate other proteins and exert biological functions.
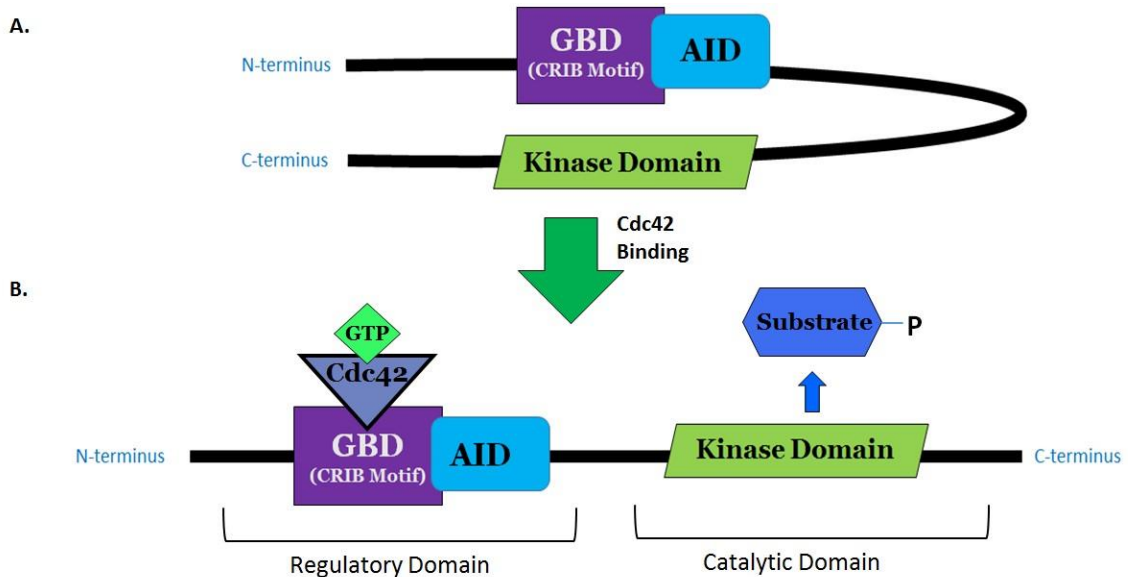
Figure 4: Inactive and active conformations of Cdc42 effector PAK. A. Schematic representation of the autoinhibited conformation of PAK protein. Interaction between the autoinhibitory domain (AID) and kinase domain prevents its activity. **B.** Functionally active, GTP-Cdc42 bound conformation of PAK protein. Binding of active Cdc42 releases the C-terminal kinase domain so that PAK may phosphorylate its substrates.

One well-studied biological function of PAK is its role in the formation of lamellipodia, membrane ruffles and actin polymerization (Figure 5). Once activated, PAK will inhibit myosin light chain kinase (MLCK) phosphorylation of myosin II regulatory light chain (MLC), which aids in the formation of lamellipodia and the disassembly of actin stress fibers and focal adhesions (Bokoch, 2003). PAK also phosphorylates LIM kinase (LIMK), which allows it to inhibit an actin capping protein known as cofilin (Sumi et al. 1999). Because cofilin binds and destabilizes actin filaments, its phosphorylation by PAK and subsequent inhibition of its function increases actin polymerization, and the formation of lamellipodia and membrane ruffles (Yang et

al. 1998, Edwards and Gill, 1999). PAK proteins have also been linked to cell survival through pathways such as phosphorylation of the PI3K/Akt pathway, which negatively regulates pro-apoptotic members of the Bcl-2 family, and inhibition of pro-apoptotic transcription factors such as Forkhead box protein (FKHR) (Radu et al. 2014, Dummler et al. 2009).

PAK protein dysregulation has proven to be pathologically relevant as well. Mutations in PAK have been observed in cognitive disorders such as MRX, and reduced PAK activity has been reported in severe Alzheimer's disease (Zhao et al. 2006). Also, aberrant PAK activity has been found to contribute to huntingtin aggregation in Huntington's disease, and in the development of fragile X syndrome in a mouse model (Ma et al. 2012). Many of these pathological findings have been attributed to Rac-PAK signaling, and as PAK is an overlapping target of both Rac and Cdc42, we chose to dedicate less focus to this signaling pathway.
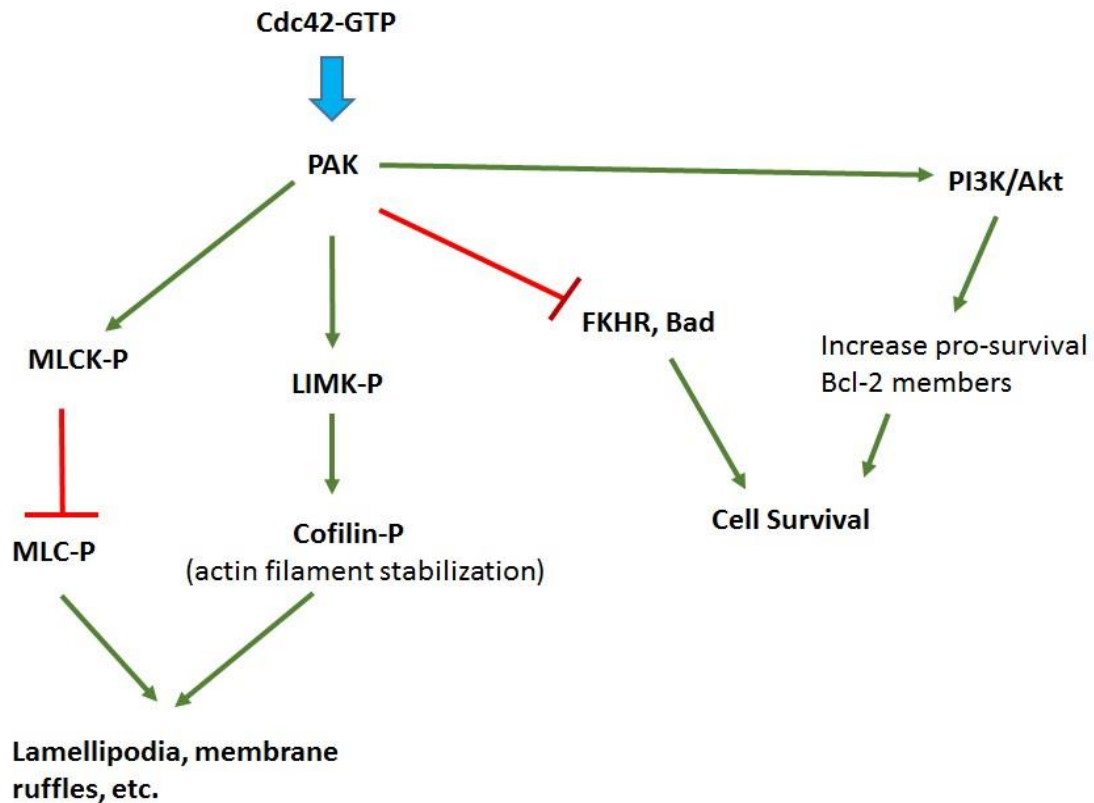
Figure 5. PAK signaling pathways involved in actin cytoskeletal regulation and cell survival. PAK activation has several actin regulatory effects, including the formation of lamellipodia and membrane ruffles. This occurs both through PAK phosphorylation of myosin light chain kinase (MLCK) and LIM kinase (LIMK), which blocks its phosphorylation of the myosin II regulatory light chain (MLC) and inhibits actin destabilizing cofilin proteins, respectively. PAK activation also supports cellular survival through inhibition of the pro-apoptotic transcription factors Forkhead box protein (FKHR) and Bad, as well as activation of the pro-survival PI3K/Akt pathway, which negatively regulates pro-apoptotic Bcl-2 family members.

1.5.3 Neuronal Wiskott-Aldrich Syndrome Protein (N-WASp)

Neuronal Wiskott-Aldrich syndrome protein (N-WASp) is the more ubiquitously expressed form of the hematopoietic protein Wiskott-Aldrich syndrome protein (WASp), both of which are dependent on direct Cdc42 binding for activation and subsequent transmission of signals to the actin cytoskeleton (Kim et al. 2000). These proteins consist of several important conserved regions (Figure 6), including a PH domain that binds PIP_2, an N-terminal GBD that contains the CRIB motif, and a C-terminal VCA (verprolin homology, cofilin homology, acidic) domain for the binding of actin monomers (V region) and association with the Arp2/3 complex (CA region) (Rohatgi et al. 1999). N-WASp also contains a basic domain (BD) which binds PIP_2, as it has been reported that signals from both Cdc42 and PIP_2 are required to adequately activate N-WASp (Prehoda et al. 2000). Finally, WASp proteins have an N-terminal domain known as WASp-homology 1 (WH1), which mediates the binding of WASp-interacting protein (WIP), which helps control cellular localization, protein stability, and protects N-WASp from degradation by ubiquitination (Fried et al. 2014, Suetsugu et al. 2002). Similar to the two aforementioned Cdc42 target proteins, inactive N-WASp also exists in an autoinhibited conformation, wherein the overlapping of the GBD and VCA domain prevents interaction with actin related proteins (Figure 6A). Upon Cdc42 binding, affinity between the GBD and VCA domains in N-WASp is reduced, and this autoinhibition is relieved (Figure 6B) (Rohatgi et al. 2000). Members of the WASp protein family can also interact with and be activated by other proteins, such as Src tyrosine kinases and adaptor proteins Nck and Grb2 (Higgs and Pollard, 1999), but these will not be further discussed here.
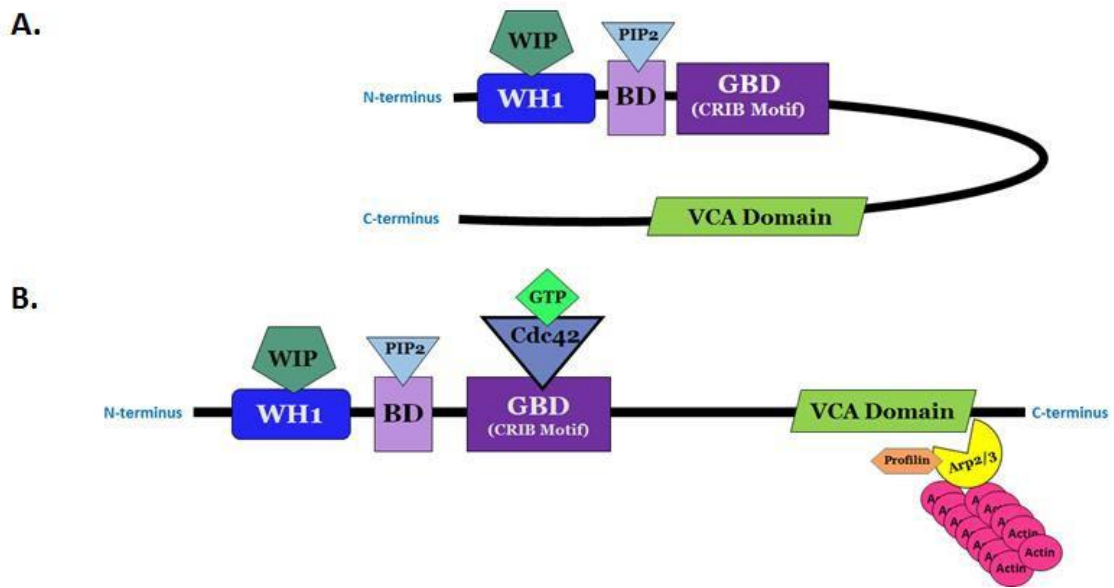
Figure 6: Inactive and active conformations of Cdc42 effector N-WASp. A. Schematic representation of autoinhibited N-WASp. Interaction between the GBD and VCA domain prevent its activity. **B.** Functionally active, GTP-Cdc42 bound conformation of N-WASp can recruit machinery to make new actin filaments.

WASp was originally identified as the protein product of a mutated gene in an immunodeficiency disorder known as Wiskott-Aldrich syndrome (WAS). The majority of mutations involved in WAS onset have been localized to the WIP-binding region, causing aberrant degradation of the protein (Fried et al. 2014). N-WASp has since been linked to this disease as a critical factor in autoimmunity development, due to its regulation of B lymphocyte signaling (Volpi et al. 2016). Figure 7 depicts a well characterized signaling pathway of N-WASp. N-WASp stimulates actin nucleation and polymerization via induction of actin related protein 2/3 (Arp 2/3) that promotes formation of actin filaments (Carlier et al. 1999, Machesky and Gould, 1999). A contribution to cell survival has not yet been described for the Cdc42-N-WASp pathway, and it is thought to serve mainly in the regulation of actin dynamics. As it is a target only

of Cdc42 GTPase, we sought to focus more on the Cdc42-N-WASp signaling pathway in

possible relation to neuronal survival.
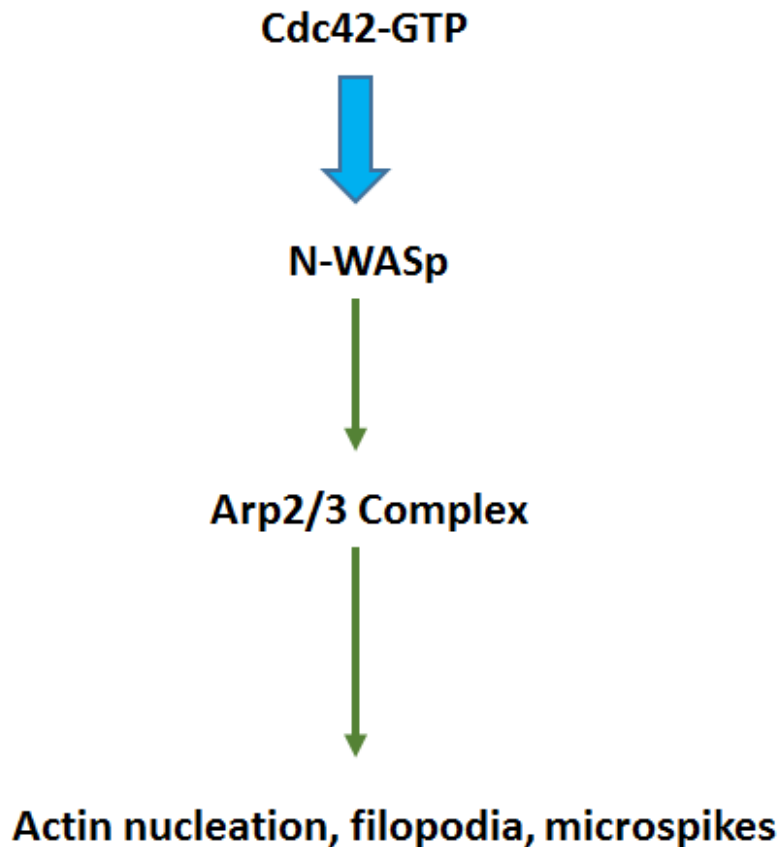
Figure 7. N-WASp signaling pathways involved in actin cytoskeletal dynamics.
Cdc42 binding and activation of N-WASp has several regulatory effects on actin
dynamics, including assisting in the development of filopodia, actin microspikes, and
actin nucleation. This occurs through N-WASp phosphorylation of the actin related
protein 2/3 (Arp2/3) complex, which regulates the formation of new actin nucleation
cores.

1.6 Cerebellar Granule Neurons (CGNs) as a Model System

Due to their relatively simple isolation process and high level of culture homogeneity (~95%), primary rat cerebellar granule neurons (CGNs) are widely used as a model system to study neuronal apoptosis (Linseman et al., 2001). Relevant to the current study, Cdc42, Rac and Rho have demonstrated strong genetic expression in various areas of the rat brain, including the hippocampus, cerebellum, thalamus and neocortex (Olenik et al. 1997). Our healthy growth medium for CGNs contained 25 mM potassium chloride (KCl), as it has been shown that this neuronal population requires high levels of extracellular calcium *in vitro,* beyond what is considered physiologically normal (D'Mello et al., 1993). This high potassium supplementation, and subsequent membrane depolarization, allows a large influx of Ca^{2+} into the cells, which is important in Ca^{2+}/Calmodulin protein kinase phosphorylation of various transcription factors and survival pathway factors (i.e., ERK, CREB). High levels of intracellular Ca^{2+} have proven important in many neuronal cell lines, including sympathetic neurons, ciliary ganglia, dorsal root ganglia and cerebellar granule neurons (Galli et al. 1995).

To induce cell stress in our model system, we chose to use 5K- media, which lacks both fetal bovine serum (FBS) and has greatly reduced potassium levels (5 mM). This reduced potassium causes membrane re-polarization, and a subsequent drop in intracellular Ca^{2+} levels. Thus, it is believed that CGNs in 5K- media culture die due to a lack of Ca^{2+} influx, and subsequent decrease in the transcription of survival proteins. CGNs exposed to low potassium containing media have been shown to undergo apoptosis through an increase in Fas death receptor binding, and the release of executioner caspase-

3 (Ginham et al, 2001), which can be visually distinguished by the presence of fragmented nuclei (D'Mello et al., 1993). This provides our experimental basis for using CGNs and 5K- media as an *in vitro* model for the involvement of Cdc42 in neuronal survival signaling pathways.

1.7 Hypothesis and Rationale

To date, most studies of the Rho GTPase family have focused on their roles in regulation of actin dynamics, which are now quite well defined. Additionally, most research has been conducted in non-neuronal cell populations. This study aimed to delineate more clearly a role for small Rho GTPase family member Cdc42 in neuronal survival and apoptosis. While previous work in healthy cell growth conditions has suggested that Cdc42 is not necessary for neuronal survival, as Rac is, to our knowledge it has not been ascertained if Cdc42 has a role in survival under cellular duress. Our study sought to determine whether or not Cdc42 contributes to neuronal survival under stressful growth conditions.

Previous studies have shown that the knockdown of Cdc42 activity using either dominant negative expression mutants, or *Clostridium difficile* Toxin B does not induce cell death under normalized conditions (Le et al. 2005). With this in mind, we aimed to determine whether functional inhibition of Cdc42 would further sensitize cells to apoptosis after the removal of both depolarizing potassium and growth factor serum with the use of 5K- media. We also studied Cdc42 downstream target proteins ACK-1, PAK

and N-WASp, in order to resolve the relative contribution of each pathway to the maintenance of cellular survival under duress.

1.8 Summary of Major Findings

Using our 5K- media stressor, which lacked both depolarizing potassium and growth factor serum, we were able to induce significant cell death compared to healthy CGNs incubated in 25K+ media. We were also able to decrease the function of Cdc42 through both pharmacological inhibition and genetic obstruction in order to explore its role in neuronal survival in arduous growth conditions. Our results indicate that the broad inhibition of Cdc42 under strenuous growth conditions does indeed further sensitize neurons to this death induced by 5K- media. Additionally, this study has provided evidence that the ACK-1 and PAK pathways are likely more relevant to neuronal survival than the N-WASp pathway. Here, we propose that dissimilar to Rac1, Cdc42 is not absolutely necessary for neuronal survival, but that it is likely an additional protective protein that could possess neuroprotective properties in stressful cellular circumstances. Our findings could introduce Cdc42 as a potential therapeutic target in slowing the advance of neurodegenerative disease, wherein neurons endure increasing levels of stress as the disease progresses.

Chapter Two: Materials and Methods

2.1 Reagents

2-(4-Bromo-2-chlorophenoxy)-*N*-[[[4-[[(4,6-dimethyl-2-pyrimidinyl)amino]sulfonyl]phenyl]amino]thioxomethyl]acetamide (ZCL278), 5,6-Diphenyl-*N*-[[(2*S*)-tetrahydro-2-furanyl]methyl]furo[2,3-*d*]pyrimidin-4-amine (AIM100), 6-(2,4-Dichlorophenyl)-8-ethyl-2-[[3-fluoro-4-(1-piperazinyl)phenyl]amino]pyrido[2,3-*d*]pyrimidin-7(8*H*)-one (FRAX486), 2-[(2,3,4,9-Tetrahydro-6-phenyl-1*H*-carbazol-1-yl)amino]ethanol (Casin), 3,6-Dibromo-*α*-[(dimethylamino)methyl]-9*H*-cabazole-9-ethanol (Wiskostatin) and 4-[4,5-Dihydro-5-(4-methoxyphenyl)-3-phenyl-1*H*-pyrazol-1-yl]benzenesulfonamide (ML141) were purchased from Tocris Bioscience (Minneapolis, MN). N-(2-chloro-6-methyl- phenyl)-2-(6-(4-(2-hydroxyethyl)- piperazin-1-yl)-2-methylpyrimidin-4- ylamino)thiazole-5-carboxamide (Dasatinib) was purchased from Selleck Chemicals LLC (Houston, TX). Cyclo(Lys-D-Phe-D-Pro-D-Phe-Phe-D-Pro-Gln)$_2$ (187-1) was purchased from Calbiochem (San Diego, CA). Basal Medium Eagle's solution, L-glutamine solution, penicillin/streptomycin solution, and fetal bovine serum (FBS) were purchased from Invitrogen (Grand Island, NY). A BCA protein assay kit was purchased from Thermo Scientific (Rockford, IL). Anti-ACK1 (phospho Y284) primary antibody, anti-Cdc42 primary antibody and anti-ACK1 primary antibody were purchased from Abcam (Cambridge, MA). Anti-active caspase 3 primary antibody was purchased from Promega Corporation (Madison, WI). Anti-β-tubulin primary antibody, Hoechst

31

33258, bovine serum albumin (BSA), p-Phenylenediamine, paraformaldehyde (PFM), leupeptin, aprotinin and thiazolyl blue tetrazolium bromide (MTT) were purchased from Sigma-Aldrich (St. Louis, MO). Fluorescein isothiocyanate (FITC) and indocarbocyanine (Cy3) conjugated secondary antibodies were purchased from Jackson ImmunoResearch Laboratories, Inc. (West Grove, PA). Secondary donkey anti-mouse and donkey anti-rabbit antibodies conjugated to horseradish peroxidase (HRP) were purchased from Bio-Rad Laboratories (Hercules, CA). Polyvinylidene difluoride (PVDF) membranes, ECL reagents and a molecular weight standard were purchased from Amersham Biosciences (Pittsburg, PA). A GTP-Cdc42 GTPase-linked immunosorbent assay (G-LISA) kit was ordered from Cytoskeleton Inc. (Denver, CO). Adenoviral constructs of Cdc42 short-hairpin RNA (shRNA) co-expressing green fluorescence protein (GFP), as well as a GFP co-expressing scrambled shRNA control adenoviral construct were purchased from Vector Biolabs (Malvern, PA).

2.2 CGN Culture and Treatment

Rat cerebellar granule neurons (CGNs) were isolated and cultured from seven-day-old Sprague-Dawley rat pups of both sexes as described previously (Linseman et al., 2001). CGNs were plated on 35-mm-diameter, six-well plastic dishes coated with poly-L-lysine, at a density of 4.0×10^6 cells/well in Basal Medium Eagle's containing 10% FBS, 25 mM potassium chloride (KCl), 2 mM L-glutamine, and penicillin-streptomycin (100 U/mL/100 µg/mL). Cytosine arabinoside (10 µM) was added to culture medium twenty-four hours after plating to limit the growth of non-neuronal cells. The CGNs were incubated in 10% CO_2 at 37℃ in culture medium for 6 to 7 days prior to

32

experimentation. With this protocol, cultures were approximately 95% pure for granule neurons.

CGNs undergoing treatment in "healthy" medium conditions remained in high potassium (25 mM KCl) culture medium containing 10% FBS. The medium for CGNs undergoing treatment in "stressful" conditions was replaced with serum-free Basal Medium Eagle's containing low-potassium (5 mM KCl). Cells were then treated with either a chemical inhibitor to Cdc42 or to one of its downstream effectors in *in vitro* concentrations derived from literature regarding previous experimentation (see Results). The *in vitro* concentrations of each inhibitor used are as follows: 50 µM ZCL278, 5 µM Casin, 10 µM ML141, 10 µM Wiskostatin, 10 µM 187-1, 10 µM AIM100, 1 µM Dasatinib and 10 µM FRAX486. For all experiments, an untreated 25K+ control and a 5K- control were used to compare cell death.

2.3 Hoechst Staining and Apoptotic Quantification

CGNs in either 25K+ or 5K- media were treated with chemical inhibitors for 24 hours as described previously prior to fixation and staining. Subsequently, the media was aspirated, CGNs were incubated for approximately 45 minutes at room temperature in 4% PFM, then washed twice with phosphate-buffered saline (PBS; pH=7.4), and finally stained with Hoechst 33258 (1 µg/mL) for visualization of DNA. Prior to imaging, the stain was removed, and PBS was added to each well. All cells were imaged using a Zeiss Axiovert-200M epifluorescence microscope. 5 DAPI images per well (in duplicate) were captured for each experiment to assay apoptosis. Cells were determined to be apoptotic based on nuclear condensation and/or fragmentation.

2.4 Immunocytochemistry and Microscopic Imaging

CGNs were co-treated in 25K+ or 5K- media for 24 hours as described previously, with or without one of the aforementioned chemical inhibitors. The cells were then washed once with PBS and fixed in 4% PFM prior to a 1 hour incubation in blocking buffer (5% BSA in 0.2% triton-X in PBS) at room temperature. This was followed by overnight incubation at 4℃ with either primary antibody against β-tubulin or primary antibody against active caspase 3, prepared in a 1:250 dilution and 1:500 dilution in 2% BSA in 0.2% triton-X in PBS, respectively. The following day, the cells were washed 5 times with PBS, and secondary antibodies were then applied for 1 hour to each well. FITC-conjugated secondary antibody was used for β-tubulin stained cells, and Cy3-conjugated secondary antibody was used for active caspase stained cells (both prepared in a 1:250 dilution in 2% BSA in 0.2% triton-X in PBS with Hoechst stain at 10 mg/mL). CGNs were then washed once more with PBS, and finally placed in p-Phenylenediamine solution to prevent photo-bleaching prior to microscopic imaging. All cells were imaged using a Zeiss Axiovert-200M epifluorescence microscope, with a minimum of 5 images captured per well (in duplicate for each treatment).

2.5 MTT Cell Viability Assay

An MTT assay was used to determine cell viability after treatment with either ZCL278 or AIM100 in both 25K+ and 5K- media conditions. CGNs were treated as described previously for 12 hours, with or without ZCL278 or AIM100. 12 mM MTT reagent was then added directly to each well (100 µL/mL), and the cells were incubated

34

at 37℃ CO_2 for 4 hours. After incubation, 4 mL of dimethyl sulfoxide (DMSO) was added to each well to solubilize any purple formazan precipitate, and the CGNs were gently rocked for approximately 1 hour at room temperature until all solid product had dissolved. 300 µL samples were then taken from each well after solubilization and re-plated (in duplicate) in a 96-well clear-bottom plate for colorimetric detection at 570 nm using Gen5 Microplate Reader spectrophotometer software. Absorbance was expressed as a percentage of the untreated control.

2.6 Cell Lysis and Protein Assays

Cell lysates were prepared and protein assays were performed prior to both Western blotting and the use of a GTPase-linked immunosorbent assay (G-LISA) kit, which will be described later on. CGNs were treated with chemical inhibitors in either 25K+ or 5K- medium as described previously for a period of 12 or 24 hours, depending on the following experiment. CGN whole cell lysates were prepared essentially as described previously (Loucks et al., 2006). Briefly, after aspiration of the media, cells were washed once with ice-cold PBS, and then incubated for 10-15 minutes in lysis buffer (Wahl buffer, leupeptin and aprotinin) prior to harvesting and a 2 minute centrifugation at 13,000 RPM. The supernatant was then taken and used to determine sample protein concentrations. Protein concentrations (µg/µL) were determined using a commercially available, colorimetric protein assay kit (BCA) and Gen5 Microplate Reader spectrophotometer software detecting at 562 nm.

2.7 GTPase-Linked Immunosorbent Assay (G-LISA)

CGNs were treated in triplicate wells with 25K+ or 5K- media for 24 hours with either ZCL278, Casin or ML141 (inhibitors to Cdc42) as described previously. Whole cell lysates were then prepared, and a protein assay was performed using the BCA colorimetric protein assay kit. All CGN lysate concentrations were equalized using ice- cold lysis buffer, and then 50 µL of either equalized lysate, buffer blank or Cdc42 positive control protein was added to replicate wells of a 96-well plate. The plate was then placed on an orbital microplate shaker at 400 RPM at 4℃ for exactly

15 minutes prior to washing and a 2 minute incubation in antigen presenting buffer for at room temperature. Another set of washes was then performed, followed by the addition of anti- Cdc42 primary antibody (diluted 1:20 in antibody dilution buffer) and a 30 minute shaking period at room temperature. After washing again, secondary antibody conjugated to HRP (diluted 1:62.5 in antibody dilution buffer) was added to each well of the plate on the orbital microplate shaker at room temperature for another 30 minutes. After a final set of washes, an HRP detection reagent mixture was added to each well, and the plate was then incubated at 37℃ for 15 minutes

before adding HRP stop buffer to each well. Sample absorbance was then immediately measured at 490 nm using Gen5 Microplate Reader spectrophotometer software.

2.8 Western Blotting

CGNs were treated in triplicate wells of 25K+ or 5K- media for 12 hours with either ZCL278 or AIM100, whole cell lysates were prepared and a protein assay was conducted, as described previously. Lysate concentrations were then equalized to the same total protein concentration (30 µg) using MilliQ water. 5X Laemmli buffer (SDS, glycerol, Tris, beta-mercaptoethanol and bromophenol blue) was then added to each sample prior to boiling in water in order to break disulfide bonds. Samples were centrifuged for 2 minutes at 13,000 RPM and kept on ice until gel loading. A 7.5% polyacrylamide gel was prepared, and each of 10 wells was filled with 1X running buffer (SDS, Tris, glycine and MilliQ water). The wells were then loaded with 125 µL of either 1X Laemmli buffer (to serve as a loading control) or equalized lysate, with one well also containing 20 µL of a molecular weight standard. The proteins were then quickly separated by electrophoresis for approximately 1 hour at 35 mA, and then more slowly overnight at 7.5 mA. The following day, a PVDF membrane was activated with methanol and rinsed with 1X transfer buffer (SDS, Tris, glycine, MilliQ water and methanol) prior to preparing the transfer stack. The proteins were then transferred to the PVDF membrane for approximately 1.5 hours before disassembling the stack and discarding the polyacrylamide gel. The membrane was then placed in blocking buffer (BSA, sodium azide and PBS-T) for 1 hour at room temperature to prevent nonspecific binding, after which a primary antibody against ACK1 (phospho Y284) was diluted 1:1000 in blocking buffer, and applied to the membrane to be incubated at 4℃ overnight. After removal of the primary antibody, the membrane was washed 3 times (15 minutes each) in phosphate-

37

buffered saline with Tween 20 (PBS-T), and a secondary antibody conjugated to HRP (rabbit, polyclonal) was diluted 1:5000 in PBS-T. The membrane was shaken in secondary antibody for approximately 2 hours, and another set of 3 PBS-T washes was performed. The membrane was then soaked in ECL reagent on a shaker at room temperature for approximately 10 minutes for luminol based detection. Hyperfilm was then exposed to the membrane for approximately 30 seconds, and the film was developed using a film processor.

2.9 Adenoviral shRNA Infection and Immunocytochemistry

CGNs were infected for 72 hours at a multiplicity of infection (MOI) of 1000 (400 x 10^7 viral particles/well) with either scrambled or Cdc42-targeted adenoviral shRNA. The virus also co-expressed green fluorescence protein (GFP), which was used to gauge the amount of cellular infection. After 48 hours of infection in 25K+ plating medium, there was a 5K- medium exchange in half of the plates treated. 24 hours later, the CGNs were fixed to the plate using 4% PFM, washed twice with PBS, and incubated in blocking buffer (triton-X and 5% BSA in PBS) for 1 hour. Afterwards, primary antibody against Cdc42 (diluted 1:200 in blocking buffer) was applied to the plates for overnight incubation at 4℃. The following day, the CGNs were washed 3 times with PBS, and a secondary antibody conjugated to Cy3 (diluted 1:250 in PBS) was applied to each well for approximately 2 hours at 4℃. After removal of the secondary antibody, the wells were washed 3 more times with PBS and placed in p-Phenylenediamine solution to prevent photo-bleaching prior to microscopic imaging. All cells were imaged using a

Zeiss Axiovert-200M epifluorescence microscope, with a minimum of 15 images

captured per well (in duplicate for each treatment).

2.10 Data Analysis

Each experiment was performed either in duplicate or triplicate wells per

treatment. Cell treatment and apoptotic quantification data were analyzed using a one-

way analysis of variance (ANOVA) with a *post hoc* Tukey's test. MTT assay and

adenoviral shRNA infection and apoptotic quantification data were analyzed using an

unpaired t-test. A p-value <0.05 was considered statistically significant. Data represent

the means ∓ standard error of the mean (SEM) for the total number (n) of experiments

performed. G-LISA data were analyzed as the mean ∓ the range of 2 sample wells

Chapter Three: Results

3.1 Cdc42 Inhibitors ZCL278, Casin and ML141, and Their Distinct Mechanisms of Action

Three pharmacologically distinct Cdc42 specific inhibitors, ZCL278, Casin and ML141, were chosen based on dissimilarities in their molecular structures (Figure 8). Experimentally used *in vitro* concentrations were derived from literature detailing preceding studies. ZCL278 directly targets the binding site for Cdc42 GEF intersectin, as well as GTP/GDP binding to inhibit Cdc42. At a concentration of 50 µM *in vitro*, ZCL278 was able to disrupt various Cdc42 directed activities (i.e.,microspike formation, neuronal branching, etc.) in both metastatic prostate PC-3 cancer cells and Swiss 3T3 fibroblasts (Friesland et al. 2013). Casin specifically inhibits PIP_2-dependent actin assembly (Peterson et al. 2006), and was found to reduce the amount of active Cdc42 in aged hematopoietic stem cells at a concentration of 5 µM *in vitro* (Florian et al. 2012). ML141 is a Cdc42 specific inhibitor with low affinity for other Rho GTPase family members (Surviladze et al. 2010). It was shown to inhibit the migratory phenotype of ovarian carcinoma cell lines OVCA429 and SKOV3ip, often attributed to Cdc42 activation, in a Boyden chamber assay at a concentration of 10 µM *in vitro* (Hong et al.

2013, Ip et al. 2011). Based on these studies, we chose to use the following *in vitro* concentrations of each inhibitor: 50 µM ZCL278, 5 µM Casin and 10 µM ML141.
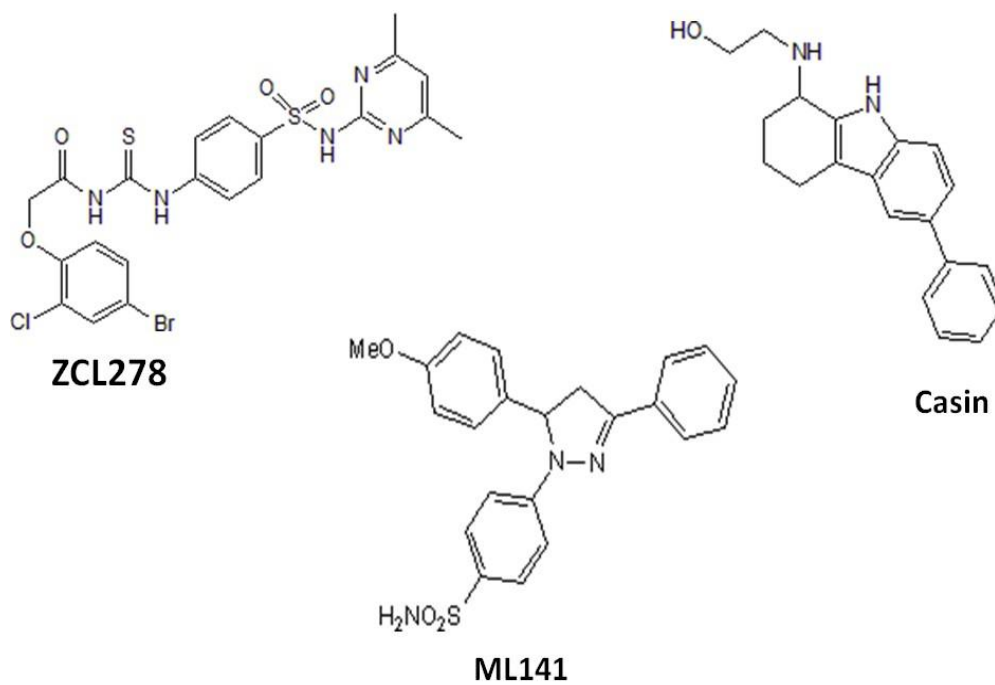
Figure 8: Distinct molecular structures of Cdc42 pharmacological inhibitors ZCL278, Casin, and ML141.

3.2 **Chemical Inhibition of Cdc42 Sensitizes CGNs to Cell Death under Stress**

CGNs were treated for 24 hours with one of the three aforementioned Cdc42 inhibitors in either 25K+ or 5K- media, and then microscopically inspected for nuclear condensation, nuclear fragmentation, and for the disruption of tubulin networking to detect apoptotic changes. By this method, it was determined that inhibition of Cdc42 activity did not significantly increase apoptosis in healthy growth medium (25K+), but did cause a substantial sensitization to apoptotic cell death upon removal of depolarizing potassium and growth factor serum (5K-). In all 25K+ treatment conditions, irrespective of inhibitor addition, apoptosis remained between 5-12%. A 5K- media exchange alone caused a significant increase in apoptosis to approximately 45-50%. Addition of Cdc42 inhibitors consistently induced an even larger increase in apoptotic cell death than in the 5K- stressful media alone.

Apoptosis in 5K- conditions increased to ~80% with the addition of ZCL278 (Figure 9), ~85% with Casin (Figure 10), and ~60% with ML141 (Figure 11). Panel A in Figures 9 and 10 depicts a negligible difference in microtubule networking amongst the cells in 25K+ media regardless of the presence of an inhibitor, and the sharp increase in damage that occurs with a 5K- media exchange accompanied by the addition of either ZCL278 or Casin. Figure 11 panel A also shows intact cellular processes, but there is no β-tubulin staining. Panel B in all 3 figures shows the changes in nuclear morphology with the addition of an inhibitor, with increasing nuclear condensation visible in the 5K- media

conditions. These results are quantitatively represented in panel C of each figure, and collectively considered with the differences in chemical structure between each inhibitor, suggest that Cdc42 likely does contribute to neuronal survival under cellular duress.
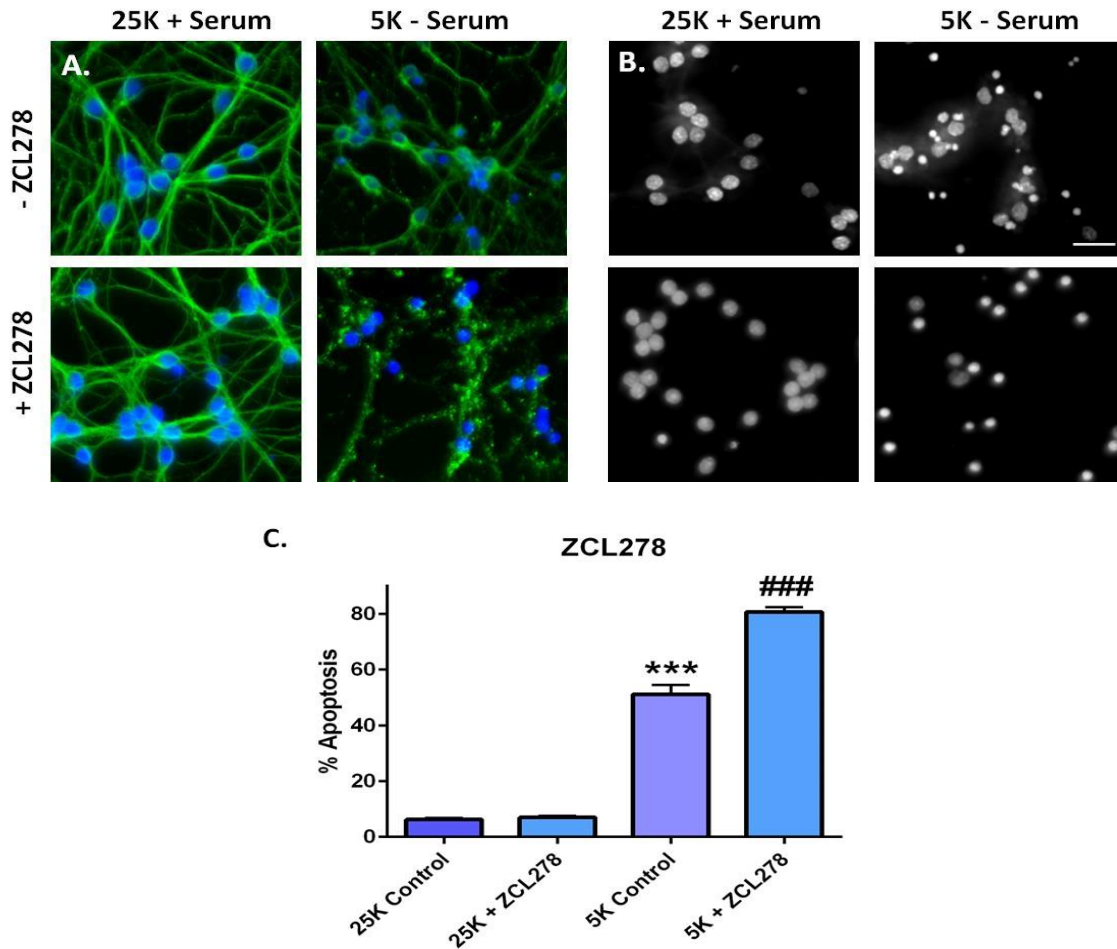
Figure 9: Apoptotic sensitization of CGNs treated with Cdc42 specific inhibitor ZCL278. A. Representative immunocytochemistry micrographs showing CGNs with or without ZCL278 treatment. Leftmost panels show ZCL278 treatment in 25K+ conditions. Rightmost panels show ZCL278 treatment in 5K- conditions. Green indicates β-tubulin. Blue indicates Hoechst staining. **B.** Representative DAPI micrographs of CGNs with or without ZCL278 treatment, showing decolorized Hoechst fluorescence to visualize nuclear morphology. Leftmost panels show ZCL278 treatment in 25K+ conditions. Rightmost panels show ZCL278 treatment in 5K- conditions. Images show 8 different fields. Scale = 10 µm **C.** Quantitative assessment of cellular apoptosis in CGNs treated with ZCL278 in both 25K+ and 5K- media conditions. Cells were counted and scored as apoptotic based on nuclear condensation and/or fragmentation, and a percentage for this group of cells was calculated. Apoptosis in the 25K+ control and 25K + ZCL278 conditions was approximately 5-10%. Apoptosis in the 5K- control increased to ~50%, and further increased in the 5K + ZCL278 condition to ~80%. Data were analyzed using one-way ANOVA and Tukey's post-hoc test. *** indicates p<0.001 compared to an untreated, 25K+ control. ### indicates p<0.001 compared to 5K- insult alone. Data are represented as the mean ± SEM, n=8.
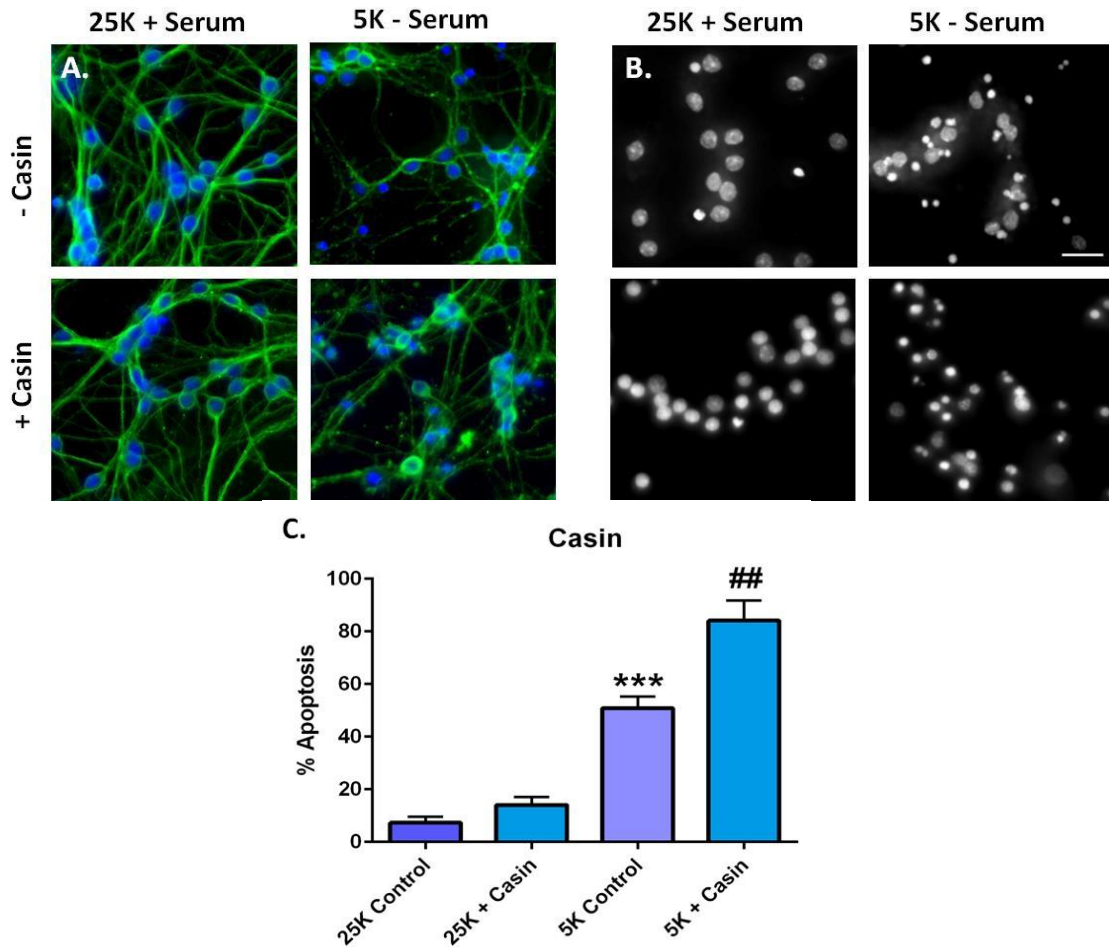
Figure 10: Apoptotic sensitization of CGNs treated with Cdc42 specific inhibitor Casin. A. Representative immunocytochemistry micrographs showing CGNs with or without Casin treatment. Leftmost panels show Casin treatment in 25K+ conditions. Rightmost panels show Casin treatment in 5K- conditions. Green indicates β-tubulin. Blue indicates Hoechst staining. **B.** Representative DAPI micrographs of CGNs with or without Casin treatment, showing decolorized Hoechst fluorescence to visualize nuclear morphology. Leftmost panels show Casin treatment in 25K+ conditions. Rightmost panels show Casin treatment in 5K- conditions. Images show 8 different fields. Scale = 10 µm **C.** Quantitative assessment of cellular apoptosis in CGNs treated with Casin in both 25K+ and 5K- media conditions. Cells were counted and scored as apoptotic based on nuclear condensation and/or fragmentation, and a percentage for this group of cells was calculated. Apoptosis in the 25K+ control and 25K + Casin conditions was approximately 7-14%. Apoptosis in the 5K- control increased to ~50%, and further increased in the 5K + Casin condition to ~85%. Data were analyzed using one-way ANOVA and Tukey's post-hoc test. *** indicates $p<0.001$ compared to an untreated, 25K+ control. ## indicates $p<0.01$ compared to 5K- insult alone. Data are represented as the mean ± SEM, n=4.
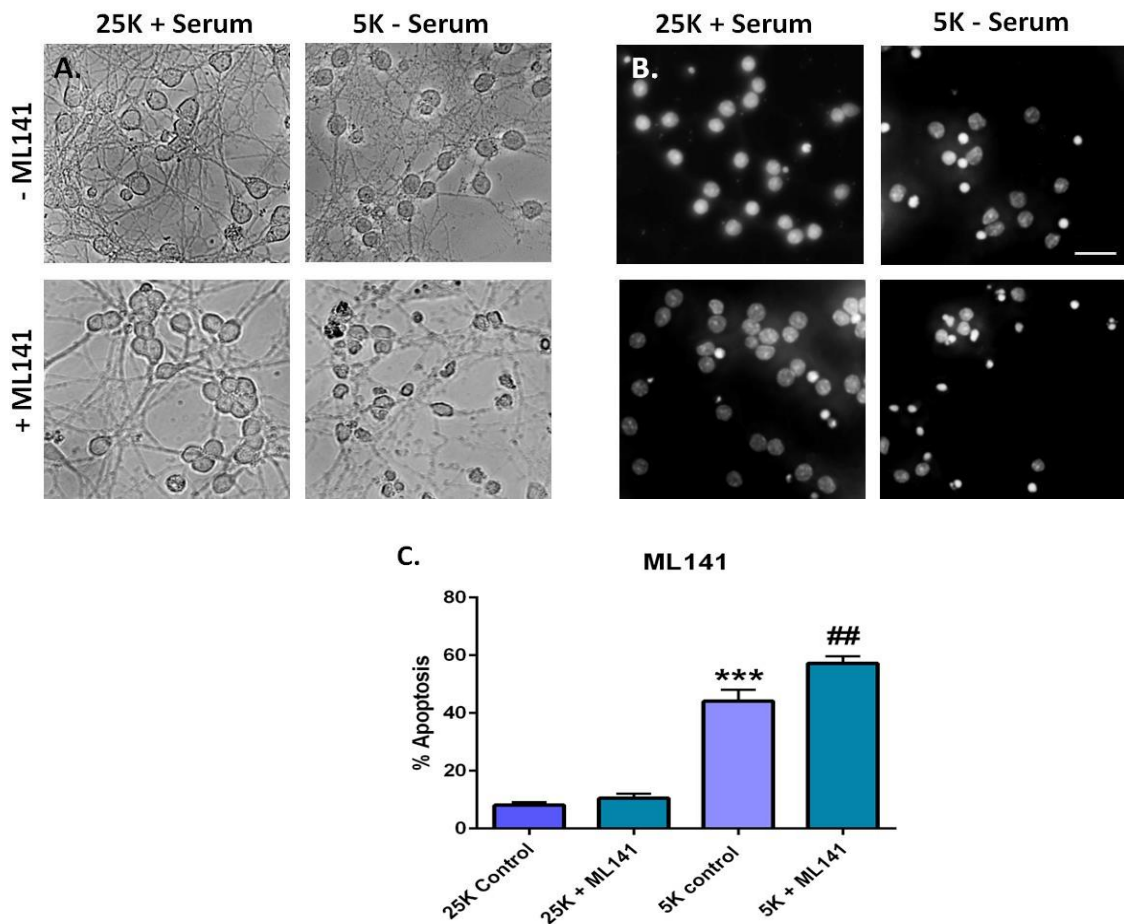
Figure 11: Apoptotic sensitization of CGNs treated with Cdc42 specific inhibitor ML141. A. Representative brightfield micrographs showing CGNs with or without ML141 treatment. Leftmost panels show ML141 treatment in 25K+ conditions. Rightmost panels show ML141 treatment in 5K- conditions. **B.** Representative DAPI micrographs of CGNs with or without ML141 treatment, showing decolorized Hoechst fluorescence to visualize nuclear morphology. Leftmost panels show ML141 treatment in 25K+ conditions. Rightmost panels show ML141 treatment in 5K- conditions. Images show 8 different fields. Scale = 10 µm. **C.** Quantitative assessment of cellular apoptosis in CGNs treated with ML141 in both 25K+ and 5K- media conditions. Cells were counted and scored as apoptotic based on nuclear condensation and/or fragmentation, and a percentage for this group of cells was calculated. Apoptosis in the 25K+ control and 25K+ ML141 conditions was approximately 8-11%. Apoptosis in the 5K- control increased to ~45%, and further increased in the 5K + ML141 condition to ~60%. Data were analyzed using one-way ANOVA and Tukey's post-hoc test. *** indicates $p<0.001$ compared to an untreated, 25K+ control. ## indicates $p<0.01$ compared to 5K- insult alone. Data are represented as the mean ± SEM, n=11.

3.3 ACK-1 Inhibitors AIM100 and Dasatinib, and their Distinct Mechanisms of Action

Two pharmacologically distinct ACK-1 specific inhibitors, AIM100 and Dasatinib, were chosen based on dissimilarities in their molecular structures (Figure 12). Experimentally used *in vitro* concentrations were derived from prior studies. X-ray crystallography and high-throughput screening studies characterized the ATP-mimicking ability, and thus ATP-site binding, of AIM100 through which it inhibits ACK-1 (DiMauro et al. 2007). AIM100 has been shown to propagate apoptosis in pancreatic cancer cell line Panc-1 at an *in vitro* concentration of 10 µM (Mahajan et al. 2012). AIM100 was also found to cause cell growth suppression in two human prostate cancer cell lines (LNCaP and LAPC4) via an increase in the quiescent G0/G1 cell phase (Mahajan et al. 2010). Dasatinib, also sold under the commercially available brand name Sprycel as an oral treatment for patients suffering from chronic myelogenous leukemia (CML), was first noted as an inhibitor of kinases such as Src and Abl (Lombardo et al. 2004). A previous chemical proteomics study in lung cancer cells demonstrated how Dasatinib inhibits ACK-1 kinase activity by decreasing four of its major sites of autophosphorylation (Tyr284, Tyr518, Tyr857 and Tyr858) (Li et al. 2010). Dasatinib was also able to decrease growth in two human malignant melanoma cell lines (HT144 and Malme-3M) at an *in vitro* concentration of 1 µM (Eustace et al. 2008). Based on these previous studies, we chose to use the following *in vitro* concentrations of each inhibitor: 10 µM AIM100 and 1 µM Dasatinib.
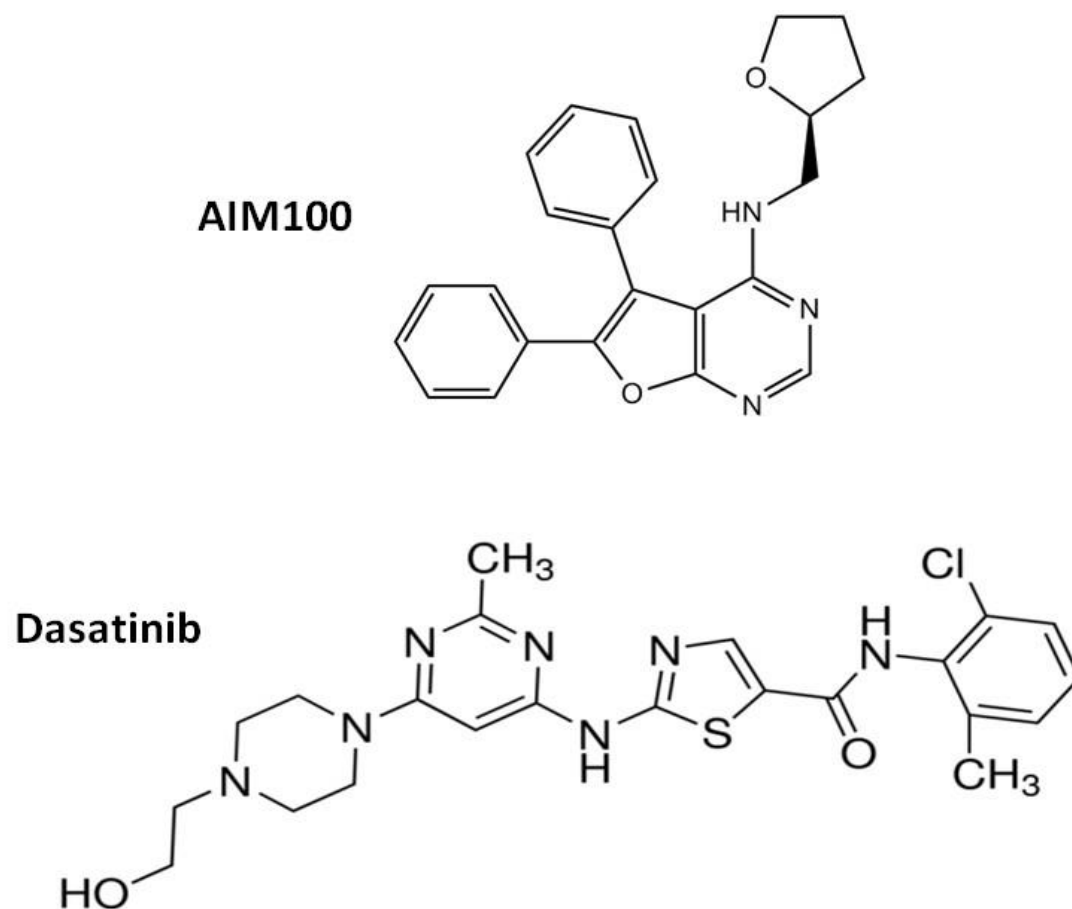
AIM100

Dasatinib

Figure 12: Distinct molecular structures of ACK-1 pharmacological Inhibitors AIM100 and Dasatinib.

3.4 **Chemical Inhibition of Downstream Effector ACK-1 Sensitizes CGNs to Cell**

Death under Stress

CGNs were treated for 24 hours with one of the two aforementioned ACK-1 specific inhibitors in either 25K+ or 5K- media, and then microscopically inspected for nuclear condensation, nuclear fragmentation, and for the disruption of tubulin networking to detect apoptotic changes. ACK-1 inhibition did not significantly increase apoptosis in healthy growth medium (25K+), but did cause a substantial sensitization to apoptotic cell death upon removal of depolarizing potassium and growth factor serum (5K-). In all 25K+ treatment conditions, irrespective of inhibitor addition, apoptosis remained between 7-12%. In all 5K- conditions without inhibitor treatment, apoptosis significantly increased to 50-60%. Inhibition of ACK-1 increased apoptotic cell death even further than in the 5K- stressful media alone.

Cell death in 5K- conditions treated with AIM100 (Figure 13) was ~90% and with Dasatinib (Figure 14) was ~80%. Figure 13 panel A shows the increase in damage to the tubulin network with the addition of AIM100 in 5K- media, and panel A in Figure 14 shows the changes in cellular processes in all treatment groups, without β-tubulin staining. Panel B in both figures depicts the increase in number of condensed/fragmented nuclei with both a 5K- media exchange, and further with the addition of either inhibitor. These results are quantitatively represented in panel C of each figure**.** Given the differences in chemical structure between each inhibitor, our results advocate an importance of the Cdc42-ACK-1 pathway in neuronal survival under cellular duress.
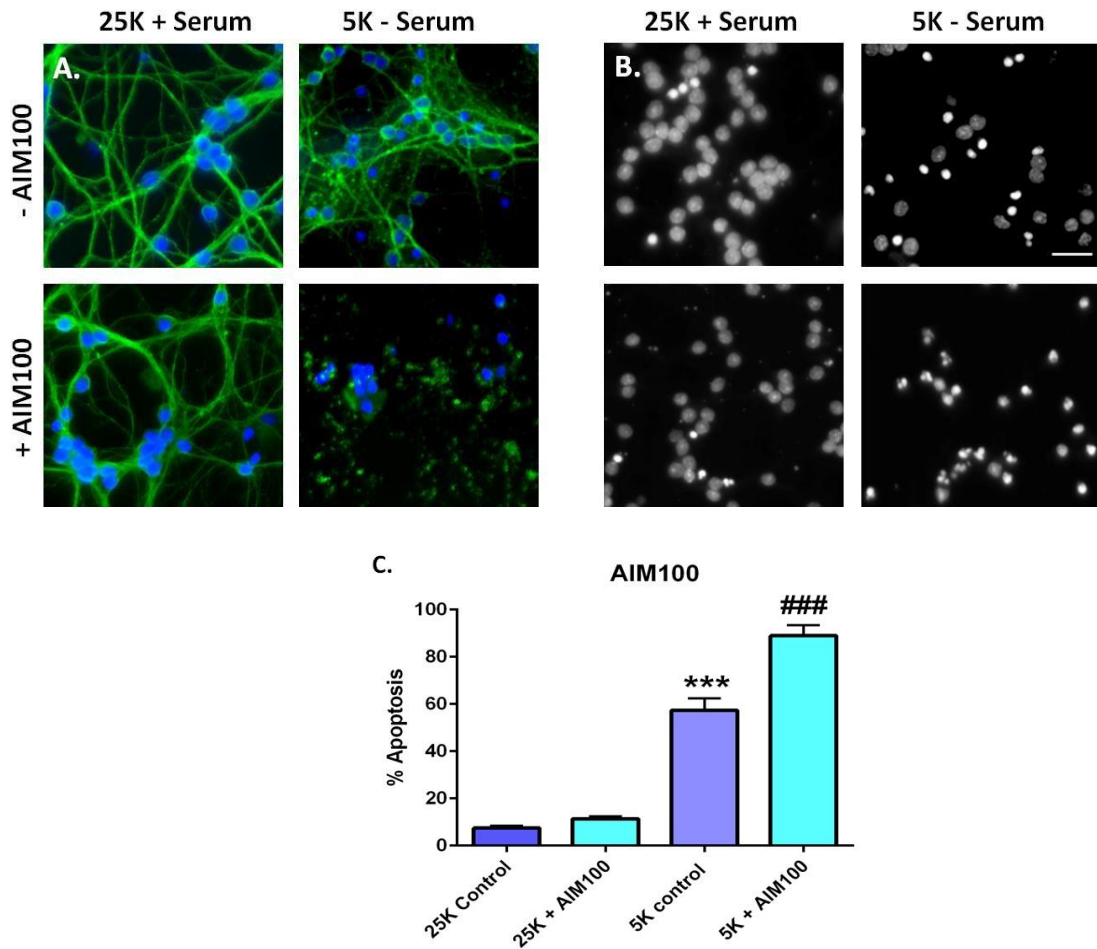
Figure 13: Apoptotic sensitization of CGNs treated with ACK-1 specific inhibitor AIM100. A. Representative immunocytochemistry micrographs showing CGNs with or without AIM100 treatment. Leftmost panels show AIM100 treatment in 25K+ conditions. Rightmost panels show AIM100 treatment in 5K- conditions. Green indicates β-tubulin. Blue indicates Hoechst staining. **B.** Representative DAPI micrographs of CGNs with or without AIM100 treatment, showing decolorized Hoechst fluorescence to visualize nuclear morphology. Leftmost panels show AIM100 treatment in 25K+ conditions. Rightmost panels show AIM100 treatment in 5K- conditions. Images show 8 different fields. Scale = 10 µm **C.** Quantitative assessment of cellular apoptosis in CGNs treated with AIM100 in both 25K+ and 5K- media conditions. Cells were counted and scored as apoptotic based on nuclear condensation and/or fragmentation, and a percentage for this group of cells was calculated. Apoptosis in the 25K+ control and 25K + AIM100 conditions was approximately 7-12%. Apoptosis in the 5K- control increased to ~60%, and further increased in the 5K + AIM100 condition to ~90%. Data were analyzed using one-way ANOVA and Tukey's post-hoc test. *** indicates $p<0.001$ compared to an untreated, 25K+ control. ### indicates $p<0.001$ compared to 5K- insult alone. Data are represented as the mean ± SEM, n=5.
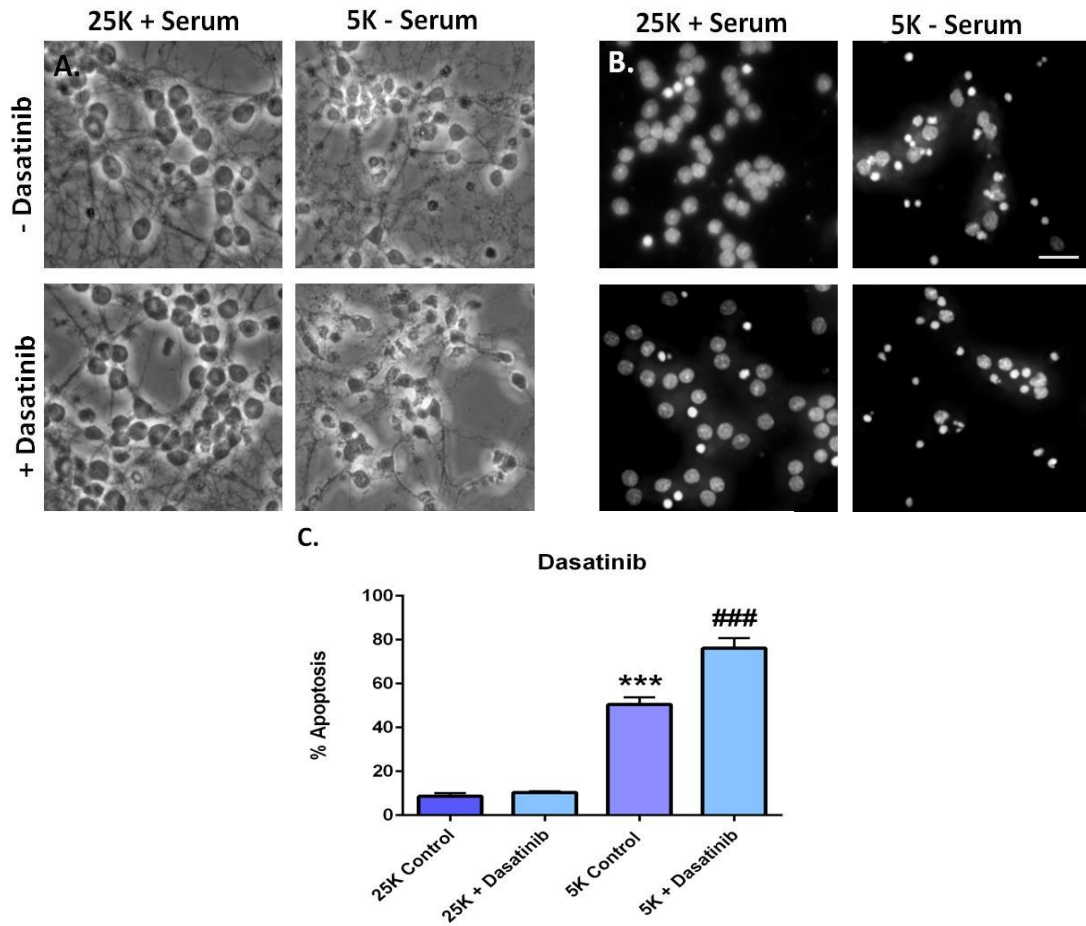
Figure 14: Apoptotic sensitization of CGNs treated with ACK-1 specific inhibitor Dasatinib. A. Representative brightfield micrographs showing CGNs with or without Dasatinib treatment. Leftmost panels show Dasatinib treatment in 25K+ conditions. Rightmost panels show Dasatinib treatment in 5K- conditions. **B.** Representative DAPI micrographs of CGNs with or without Dasatinib treatment, showing decolorized Hoechst fluorescence to visualize nuclear morphology. Leftmost panels show Dasatinib treatment in 25K+ conditions. Rightmost panels show Dasatinib treatment in 5K- conditions. Images show 8 different fields. Scale = 10 µm **C.** Quantitative assessment of cellular apoptosis in CGNs treated with Dasatinib in both 25K+ and 5K- media conditions. Cells were counted and scored as apoptotic based on nuclear condensation and/or fragmentation, and a percentage for this group of cells was calculated. Apoptosis in the 25K+ control and 25K + Dasatinib conditions was approximately 8-10%. Apoptosis in the 5K- control increased to ~50%, and further increased in the 5K + Dasatinib condition to ~80%. Data were analyzed using one-way ANOVA and Tukey's post-hoc test. *** indicates $p<0.001$ compared to an untreated, 25K+ control. ### indicates $p<0.001$ compared to 5K- insult alone. Data are represented as the mean ± SEM, n=6.

3.5 **PAK Inhibitor FRAX486 and its Mechanism of Action**

The chemical inhibitor specific to Cdc42 downstream effector PAK chosen was

FRAX486 (Figure 15), and an experimental *in vitro* concentration was determined from

prior studies. FRAX486 was seen to inhibit Group I PAKs (PAKs 1-3) in an *in vitro*

kinase assay (Dolan et al. 2013). It was also able to cause actin filament degeneration in a

concentration dependent manner (1-10 µM) in human prostatic stromal myofibroblast

cell line WPMY-1 (Wang et al. 2016). As PAK is a common protein target of both Cdc42

and Rac GTPases, there have been many FRAX486 studies conducted to delineate its

effects in Rac pathways. For example, one schizophrenia study found that the blocking of

PAK by FRAX486 actually prevents dendritic spine destruction caused by overactive

Rac1 and downregulated *DISC1,* which is a gene that helps regulate cerebral cortex

neurons (Hayashi-Takagi et al. 2014). Based on these previous studies, we chose to use

an *in vitro* concentration of 10 µM FRAX486.
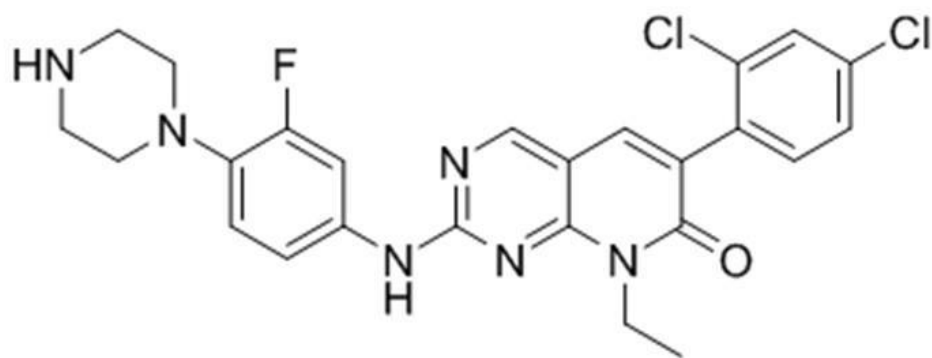
FRAX486

Figure 15: Molecular structure of PAK pharmacological inhibitor FRAX486.

3.6 **Chemical Inhibition of Downstream Effector PAK Sensitizes CGNs to Cell Death under Stress**

CGNs were treated for 24 hours with FRAX486 in either 25K+ or 5K- media, and then microscopically inspected for nuclear condensation, nuclear fragmentation, and for the disruption of tubulin networking to detect apoptotic changes. PAK inhibition did not significantly increase apoptosis in healthy growth medium (25K+), but did cause a substantial sensitization to apoptotic cell death upon removal of depolarizing potassium and growth factor serum (5K-). In all 25K+ treatment conditions, irrespective of inhibitor addition, apoptosis remained between 5-10%. In all 5K- conditions without inhibitor treatment, apoptosis significantly increased to 40%. Inhibition of PAK increased apoptotic cell death even further than in the 5K- stressful media alone.

PAK specific chemical inhibitor FRAX486 induced apoptosis at ~80% in the 5K-media (Figure 16). In this figure, panel A shows the negligible difference in microtubule networking amongst the cells incubated in 25K+ media, regardless of PAK inhibition, and the harsh destruction of it after a 5K- media exchange and FRAX486 treatment. Panel B depicts the increase in cell death seen with a 5K- media exchange alone, and even further with the addition of FRAX486 based on the number of condensed or fragmented nuclei. These results are quantitatively represented in panel C, and suggest a role for the Cdc42-PAK pathway in neuronal survival. However, it is important to note that PAK is also a downstream target of Rac, which has well defined roles as a pro-survival protein in neurons. Therefore these results were somewhat expected, and this pathway was not explored as extensively.

53
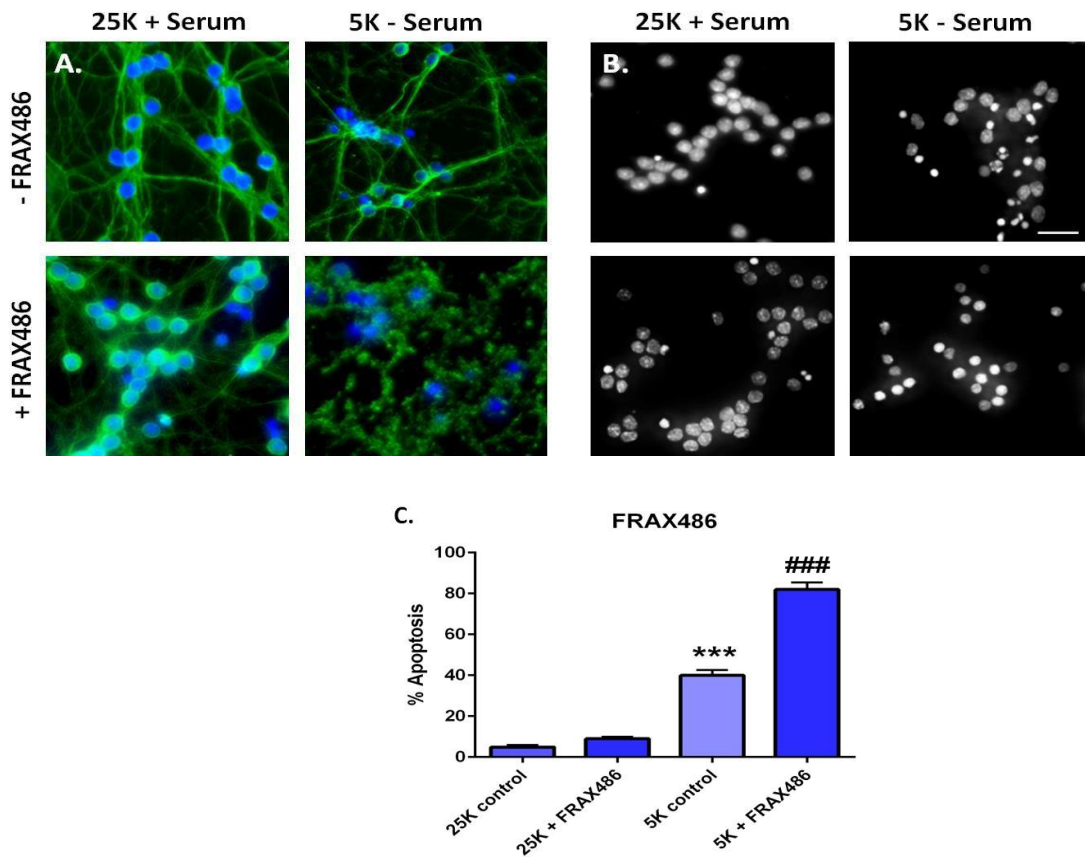
Figure 16: Apoptotic sensitization of CGNs treated with PAK specific inhibitor FRAX486. A. Representative immunocytochemistry micrographs showing CGNs with or without FRAX486 treatment. Leftmost panels show FRAX486 treatment in 25K+ conditions. Rightmost panels show FRAX486 treatment in 5K- conditions. Green indicates β-tubulin. Blue indicates Hoechst staining. **B.** Representative DAPI micrographs of CGNs with or without FRAX486 treatment, showing decolorized Hoechst fluorescence to visualize nuclear morphology. Leftmost panels show FRAX486 treatment in 25K+ conditions. Rightmost panels show FRAX486 treatment in 5K- conditions. Images show 8 different fields. Scale = 10 µm **C.** Quantitative assessment of cellular apoptosis in CGNs treated with FRAX486 in both 25K+ and 5K- media conditions. Cells were counted and scored as apoptotic based on nuclear condensation and/or fragmentation, and a percentage for this group of cells was calculated. Apoptosis in the 25K+ control and 25K + FRAX486 conditions was approximately 5-10%. Apoptosis in the 5K- control increased to ~40%, and further increased in the 5K + FRAX486 condition to ~80%. Data were analyzed using one-way ANOVA and Tukey's post-hoc test. *** indicates p<0.001 compared to an untreated, 25K+ control. ### indicates p<0.001 compared to 5K- insult alone. Data are represented as the mean ± SEM, n=7.

3.7 N-WASp Inhibitors 187-1 and Wiskostatin, and their Distinct Mechanisms of Action

Two pharmacologically distinct N-WASp specific inhibitors, 187-1 and Wiskostatin, were chosen based on dissimilarities in their molecular structures (Figure 17). Experimentally used *in vitro* concentrations were determined from prior studies. 187-1 is a 14-amino acid cyclic peptide that maintains N-WASp in its autoinhibited conformation, and was found to reduce cellular migration and invasion in patients with rheumatoid arthritis (Connolly et al. 2011, Biro et al. 2014). It was also able to inhibit PIP_2-induced actin assembly at *in vitro* concentrations lower than 10 µM (Peterson et al. 2001, Hofmann et al. 2000). Wiskostatin binds the GBD of N-WASp, stabilizing it in its autoinhibited conformation. Consequently, the C-terminal VCA domain can no longer bind monomeric actin or the Arp2/3 complex, thus blocking initiation of new actin filament formation (Peterson et al. 2004, Guerriero and Weisz, 2007). In one study of hippocampal neurons, both RNA interference (RNAi) and the use of Wiskostatin caused a similar reduction in dendritic spine density and in the number of excitatory synapses (Wegner et al. 2008). Another study of two lung cancer cell lines (A-549 and SK-MES-1) demonstrated how Wiskostatin treatment decreased their invasive capacity, as well as the overall amount of paxillin rich adhesions in each cell type (Frugtniet et al 2017). At a concentration of 10 µM *in vitro,* Wiskostatin was found to block formation of dorsal ruffles in mouse embryonic fibroblasts (MEFs) (Legg et al. 2007). Based on these

previous studies, we chose to use an *in vitro* concentration of 10 µM for both 187-1 and

Wiskostatin.
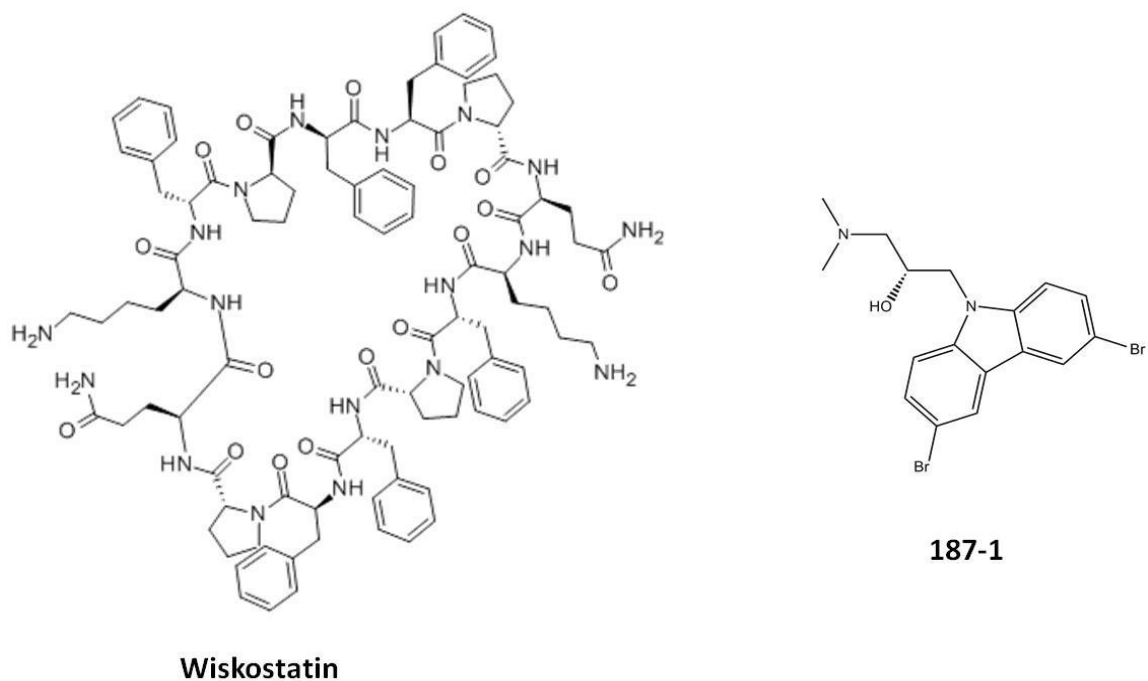
Wiskostatin

187-1

Figure 17: Distinct molecular structures of N-WASp pharmacological Inhibitors 187-1 and Wiskostatin.

3.8 **Chemical Inhibition of Downstream Effector N-WASp Does Not Sensitize CGNs to Cell Death under Stress**

CGNs were treated for 24 hours with one of the two aforementioned N-WASp chemical inhibitors in either 25K+ or 5K- media, and then microscopically inspected for nuclear condensation, nuclear fragmentation, and for the disruption of tubulin networking to detect apoptotic changes. N-WASp inhibition did not significantly increase apoptosis in either 25K+ or 5K- conditions. In all 25K+ treatment conditions, irrespective of inhibitor addition, apoptosis remained between 7-12%. In all 5K- conditions without inhibitor treatment, apoptosis significantly increased to 45-50%. Addition of either 187-1 (Figure 18) or Wiskostatin (Figure 19) only increased cell death to ~50% and ~60%, respectively. Although slight changes in nuclear morphology and neuronal processes were noted, the overall increase in apoptosis was not considered statistically significant, as quantitatively represented in panel C of both figures. These results suggest that, dissimilar to the other Cdc42 downstream target proteins, N-WASp likely does not play a substantial role in neuronal survival.
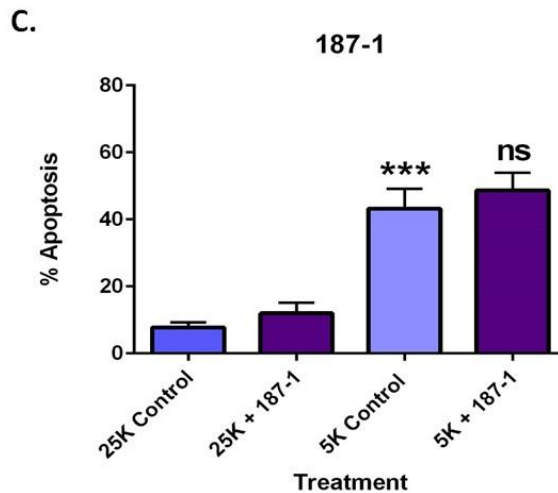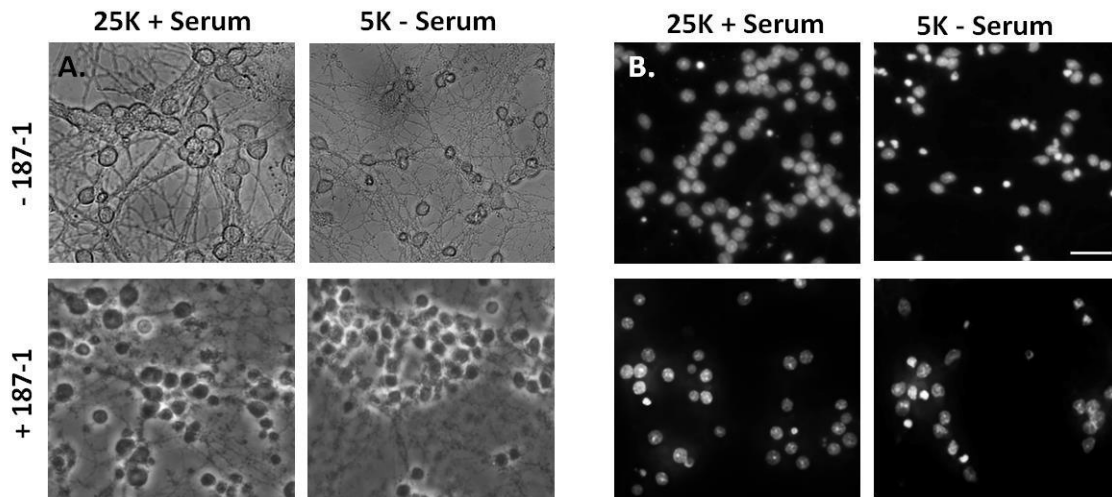
Figure 18: Apoptotic quantification of CGNs treated with N-WASp specific inhibitor 187-1. A. Representative brightfield micrographs showing CGNs with or without 187-1 treatment. Leftmost panels show 187-1 treatment in 25K+ conditions. Rightmost panels show 187-1 treatment in 5K- conditions. **B.** Representative DAPI micrographs of CGNs with or without 187-1 treatment, showing decolorized Hoechst fluorescence to visualize nuclear morphology. Leftmost panels show 187-1 treatment in 25K+ conditions. Rightmost panels show 187-1 treatment in 5K- conditions. Images show 8 different fields. Scale = 10 µm **C.** Quantitative assessment of cellular apoptosis in CGNs treated with 187-1 in both 25K+ and 5K- media conditions. Cells were counted and scored as apoptotic based on nuclear condensation and/or fragmentation, and a percentage for this group of cells was calculated. Apoptosis in the 25K+ control and 25K + 187-1 conditions was approximately 8-12%. Apoptosis in the 5K- control increased to ~45%, and only slightly increased in the 5K + 187-1 condition to ~50%. Data were analyzed using one-way ANOVA and Tukey's post-hoc test. *** indicates p<0.001 compared to an untreated, 25K+ control. Data are represented as the mean ± SEM, n=4.
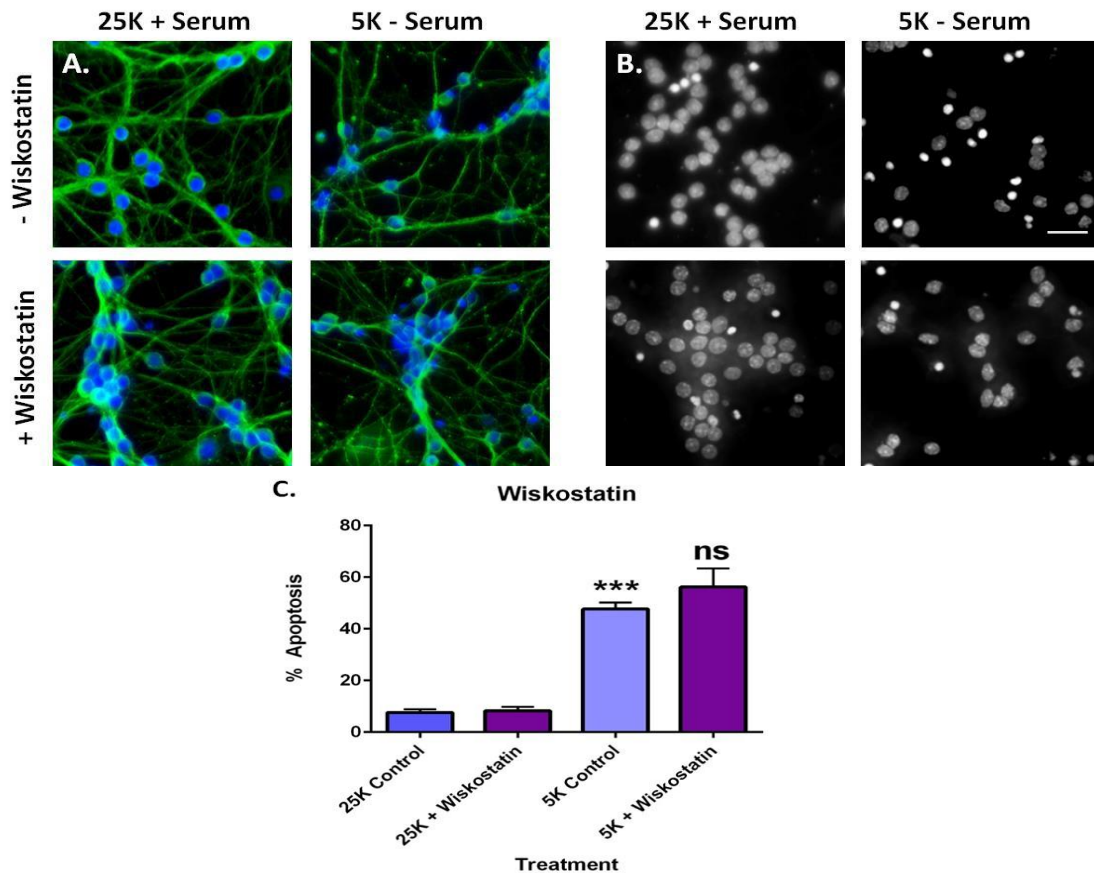
Figure 19: Apoptotic quantification of CGNs treated with N-WASp specific inhibitor Wiskostatin. A. Representative immunocytochemistry micrographs showing CGNs with or without Wiskostatin treatment. Leftmost panels show Wiskostatin treatment in 25K+ conditions. Rightmost panels show Wiskostatin treatment in 5K-conditions. Green indicates β-tubulin. Blue indicates Hoechst staining. **B.** Representative DAPI micrographs of CGNs with or without Wiskostatin treatment, showing decolorized Hoechst fluorescence to visualize nuclear morphology. Leftmost panels show Wiskostatin treatment in 25K+ conditions. Rightmost panels show Wiskostatin treatment in 5K- conditions. Images show 8 different fields. Scale = 10 µm **C.** Quantitative assessment of cellular apoptosis in CGNs treated with Wiskostatin in both 25K+ and 5K-media conditions. Cells were counted and scored as apoptotic based on nuclear condensation and/or fragmentation, and a percentage for this group of cells was calculated. Apoptosis in the 25K+ control and 25K + Wiskostatin conditions was approximately 7-8%. Apoptosis in the 5K- control increased to ~50%, and only slightly increased in the 5K + Wiskostatin condition to ~60%. Data were analyzed using one-way ANOVA and Tukey's post-hoc test. *** indicates $p<0.001$ compared to an untreated, 25K+ control. Data are represented as the mean ± SEM, n=6.

3.9 **The Efficacy of Cdc42 Inhibitors ZCL278, Casin and ML141, and ACK-1 Inhibitor AIM100**

Although microscopic imaging and analyses were performed to assess inhibitor function, we wanted to confirm the efficacy of our chemical inhibitors using other experimental methods. An enzyme-linked immunosorbent assays (ELISA) is a colorimetric assay that can be used to detect the amount of a specific protein within a sample, by utilizing antibody binding and substrate activity to assess that protein's activity. A GTPase-linked immunosorbent assay (G-LISA) was performed to determine the efficacy of inhibitors ZCL278, Casin and ML141 in decreasing the amount of active (GTP-bound) Cdc42 in CGN samples. 24-hour treatment with the inhibitors decreased GTP-Cdc42 in samples that were incubated in 5K- media. There was no apparent difference in the amount of active Cdc42 between the 25K+ and 5K- control samples, indicating that the inhibitors were responsible for the decrease in active Cdc42.
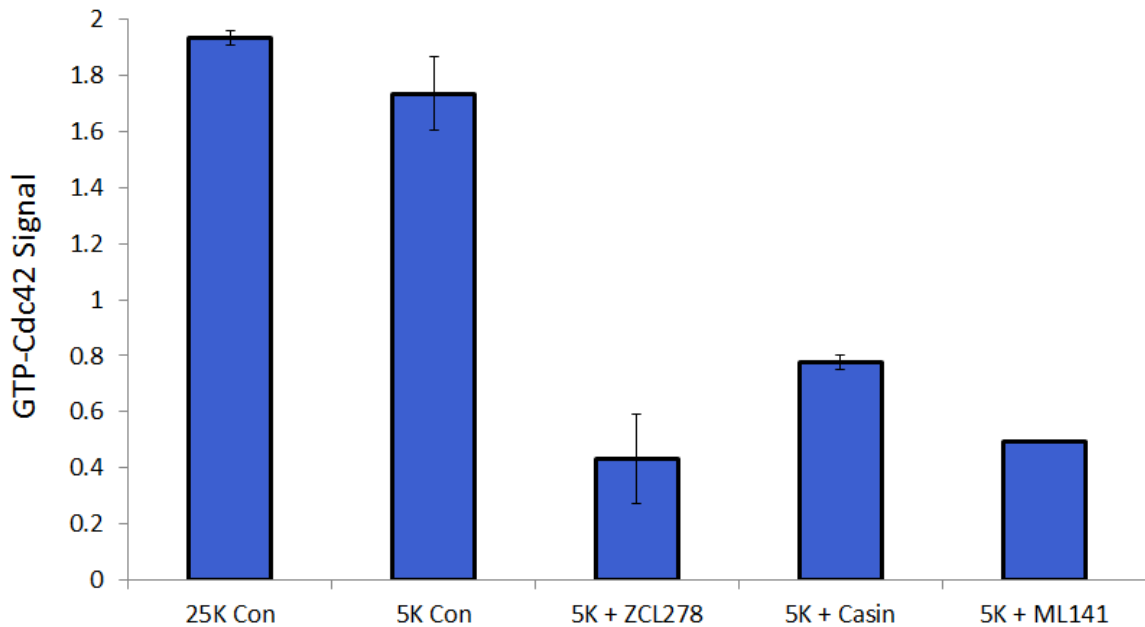
Figure 20: Detection of active Cdc42 after chemical inhibition. Representative G-LISA data of CGNs treated with Cdc42 specific inhibitors ZCL278, Casin and ML141 for 24 hours in either 25K+ or 5K- media. Data are represented as the mean ∓ the range of duplicate samples from a single experiment.

In an attempt to conserve both time and experimental materials, we chose to focus on two specific inhibitors. ZCL278 and AIM100 were chosen as representative inhibitors based on their ability to consistently block Cdc42 and ACK-1 function, respectively. Also, ACK-1 was a pathway of intense focus because it is solely a target of Cdc42 GTPase, and has been implicated in cell survival (see Introduction). As mentioned previously, ACK-1 is a non-receptor tyrosine kinase, and thus functions to phosphorylate both itself and other substrates. Therefore, we chose to conduct a Western blot for phosphorylated and total ACK-1 after a 12 hour incubation with ZCL278 and AIM100 in order to observe their inhibitory capacity. Western blots utilize several different qualities of proteins (i.e., size, antibody-binding, charge), and can be used to determine if a

particular sample contains a protein of interest. Figure 21 shows that the amount of

phosphorylated ACK-1 decreased in the 5K- samples treated with both ZCL278 and

AIM100. The amount of total ACK-1, however, did not change between each treatment,

indicating that each well was loaded with the same amount of total protein. These results

also suggest that the chemical obstruction of Cdc42 or, more directly of ACK-1 itself, is

accomplished by decreasing the phosphorylation (activation) of ACK-1, rather than

causing its degradation or loss.
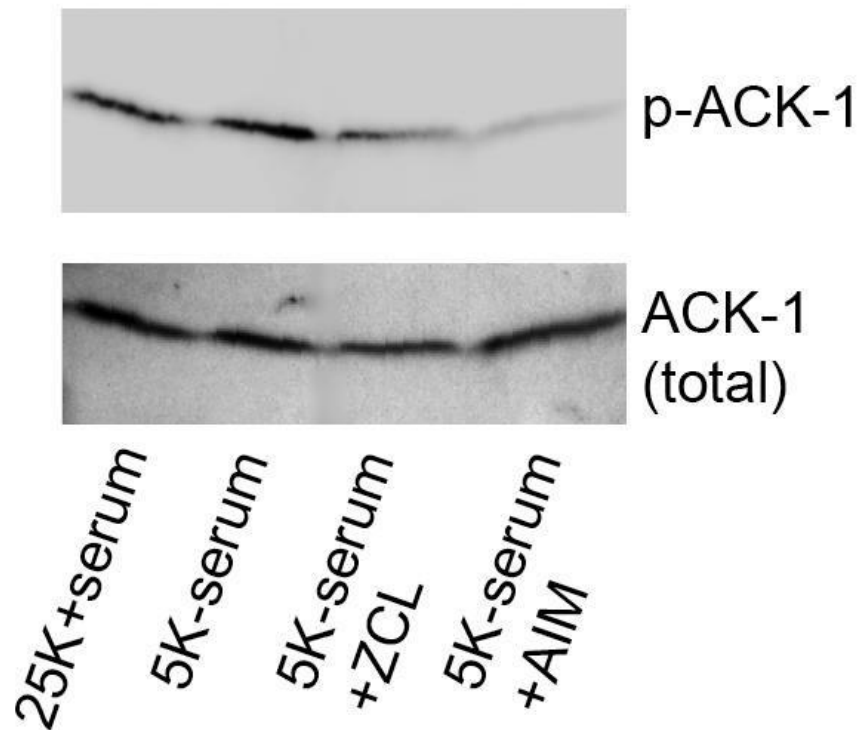
Figure 21: Detection of phosphorylated and total ACK-1 protein after chemical inhibition. Representative Western blot for detection of both phosphorylated ACK-1 (phospho Y284) and total ACK-1 (to serve as a loading control) after 12 hours of treatment with either ZCL278 or AIM100. Note the apparent decrease in band density in p-ACK-1 for the 5K- media conditions treated with either inhibitor.

3.10 **Confirmation of Cell Death as a Measure of Metabolic Function and Release of**

Active Caspase-3

Changes in nuclear morphology are an indicator of apoptotic cell death, however they are not alone sufficient to say that death is indisputable. To confirm that CGNs were actually dying in the presence of chemical inhibitors ZCL278 and AIM100 both MTT assays and active caspase-3 staining were performed. An MTT tetrazolium reduction assay measures cell viability as a function of metabolic activity and mitochondrial function. When MTT reagent is added to a culture sample, it is initially yellow in color, and mitochondrial enzymes in living cells will convert the MTT to a purple formazan product (Riss et al. 2015). In the absence of living cells, MTT reagent will remain yellow, indicating that cell death has occurred. Mitochondrial function is also pertinent to apoptotic pathway induction, as its release of cytochrome C into the cytosol is what drives the activation of caspase cascades. Caspase-3, also known as the executioner caspase, is what triggers cell death in both intrinsic and extrinsic apoptosis, and thus its activation is a clear indicator that cell death is transpiring (Bressenot et al. 2009).

To perform an MTT assay, we treated CGNs with either ZCL278 or AIM100 for approximately 12 hours prior to a 4 hour incubation period with MTT reagent. Afterwards, changes in absorbance were detected at 570 nm and expressed as a percentage of an untreated 25K+ control (Figure 22). Figure 22A shows the conversion of MTT to purple formazan product in all 25K+ conditions, but a decrease in color change in the 5K- samples, with virtually no change apparent in either 5K- + ZCL278 or 5K- + AIM100. Figures 22B and 22C quantitatively show that while there was a significant

reduction in cell viability with a 5K- media exchange alone (~40% viability), both

ZCL278 and AIM100 decreased cell viability further to below 10%. This indicates that

the 5K- media alone could successfully induce significant cell death, and inhibition of

Cdc42 or ACK-1 using ZCL278 and AIM100, respectively, substantially sensitized the

CGNs further to apoptosis.
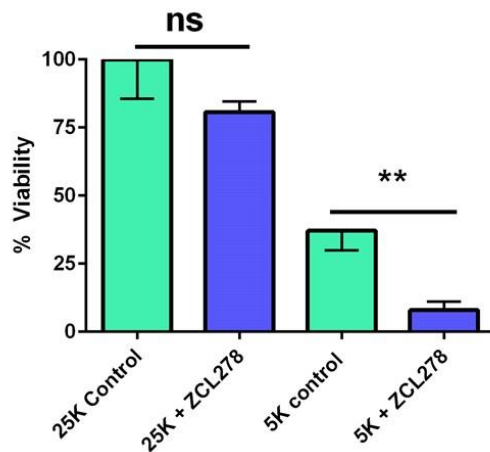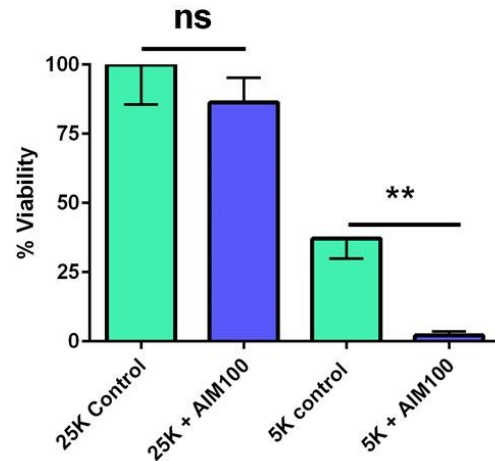
Figure 22: Assessment of cell viability as a function of mitochondrial function in CGNs treated with ZCL278 and AIM100. Quantification of cell viability as a measure of mitochondrial function in cells treated with chemical inhibitors. **A,** Representative MTT assay image of CGNs in either 25K+ or 5K- media that have been treated with ZCL278 or AIM100. Note the purple color in 25K+ conditions, and yellow color in 5K- conditions. **B-C,** Quantification of cell viability as a function of MTT assay data. The difference in viability between the 25K+ control (~100%) and 25K+ ZCL278 (~80%) or 25K+ AIM100 (~85) treated cells was not significant. The difference in cell viability between the 5K- control (~40%) and 5K- with ZCL278 (~8%) or AIM100 (~2%) treated cells was statistically significant. Data was analyzed using an unpaired t-test. ** indicates p<0.01 compared to the 5K- insult alone, n=5.

65

For immunocytochemistry detection of active caspase-3, CGNs were treated for 24 hours with either ZCL278 or AIM100 prior to staining for active caspase-3 (Figure 23). Panels A and B illustrate the caspase activation that occurred due to a 5K- media alone, and that there was no caspase activity observed in the 25K+ conditions. With the addition of either ZCL278 (Figure 23C and 23D) or AIM100 (Figure 23E and 23F), caspase activation is also more prominent in the 5K- media than in the 25K+ media conditions. White arrows indicate the presence of active caspase-3. These results collectively suggest that cell death is evident in the 5K- media conditions, and can be further propagated by inhibiting Cdc42 and ACK-1.
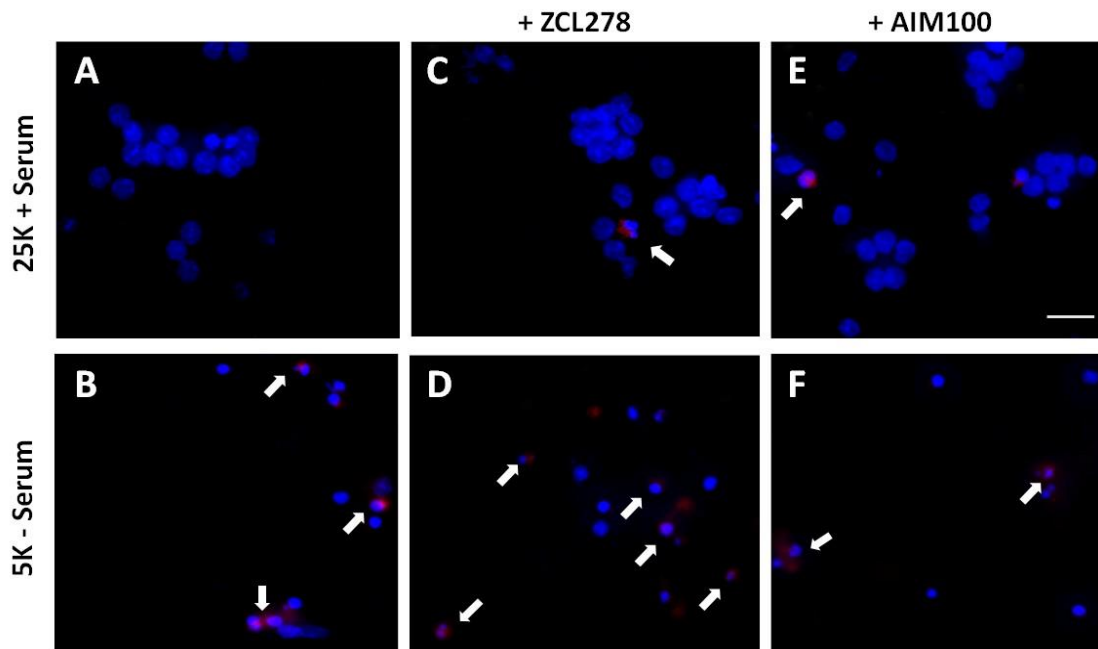
Figure 23: Active-caspase 3 release in CGNs treated with ZCL278 and AIM100. A. Representative micrograph of untreated, 25K+ control sample CGNs. **B.** Representative micrograph of 5K- insult alone control sample CGNs. **C.** Representative micrograph of caspase activation in 25K+ZCL278 treated CGNs. **D.** Representative micrograph of caspase activation in 5K- sample CGNs treated with ZCL278. **E.** Representative micrograph of caspase activation in 25K+AIM100 treated CGNs. **F.** Representative micrograph of caspase activation in 5K- sample CGNs treated with AIM100. Blue fluorescence indicates chromatin, red fluorescence indicates caspase-3 activation. Images show 6 separate fields. Scale = 10 µm. White arrows indicate apoptotic cells releasing caspase-3.

3.11 **Genetic Obstruction of Cdc42 Function Propagates Cell Death under Duress**

Chemical Inhibition is a useful preliminary tool for defining the function of a gene or protein, but more molecular approaches must be conducted for conclusive evidence. RNA interference methods are often used to silence the expression of certain genes, and thus limit the expression of certain proteins to delineate their function. Short-hairpin RNA (shRNA) is an RNA interference technique wherein a small, double-stranded RNA molecule is delivered into a cell nucleus and binds its complimentary target mRNA sequence to cause its degradation or functional inactivation (O'Keefe, 2013). Delivery of shRNA to the cell nucleus can be accomplished with the use of bacterial or viral expression vectors, and once inside the nucleus, shRNA will integrate into the cellular genome and terminate target gene expression through induction of endogenous RNA-induced silencing complex (RISC) and endonucleases (Taxman et al. 2010). To serve as a control, the target shRNA nucleotide sequence will also be "scrambled", or randomly rearranged so that it does not bind the target mRNA, and thus will not silence genetic function in the gene of interest.

In order to definitively determine the role of Cdc42 in neuronal survival under stress, we infected CGNs with an adenoviral expression vector of Cdc42 targeting shRNA. This viral construct also co-expressed green fluorescence protein (GFP), which enabled us to determine whether adequate cellular infection was achieved. CGNs were incubated with the adenovirus at a multiplicity of infection (MOI) of 1000 (400 x 10^7 viral particles/well) in 25K+ culture media for an initial 48 hour time period, before performing a 5K- media exchange. After 24 hours of 5K- media exposure (72 hours total

viral infection), the CGNs were fixed and stained for the presence of Cdc42, and

quantified for apoptosis. Figure 24 shows the efficacy of adenoviral infection after 48

hours (the time point at which the 5K- media stressor was introduced), and Figure 25

shows the percentage of GFP-expressing, virally infected cells that were quantified In

both scrambled and target shRNA infected cell groups. Note the white arrows, which

indicate cells that were infected with either scrambled or target Cdc42 shRNA.
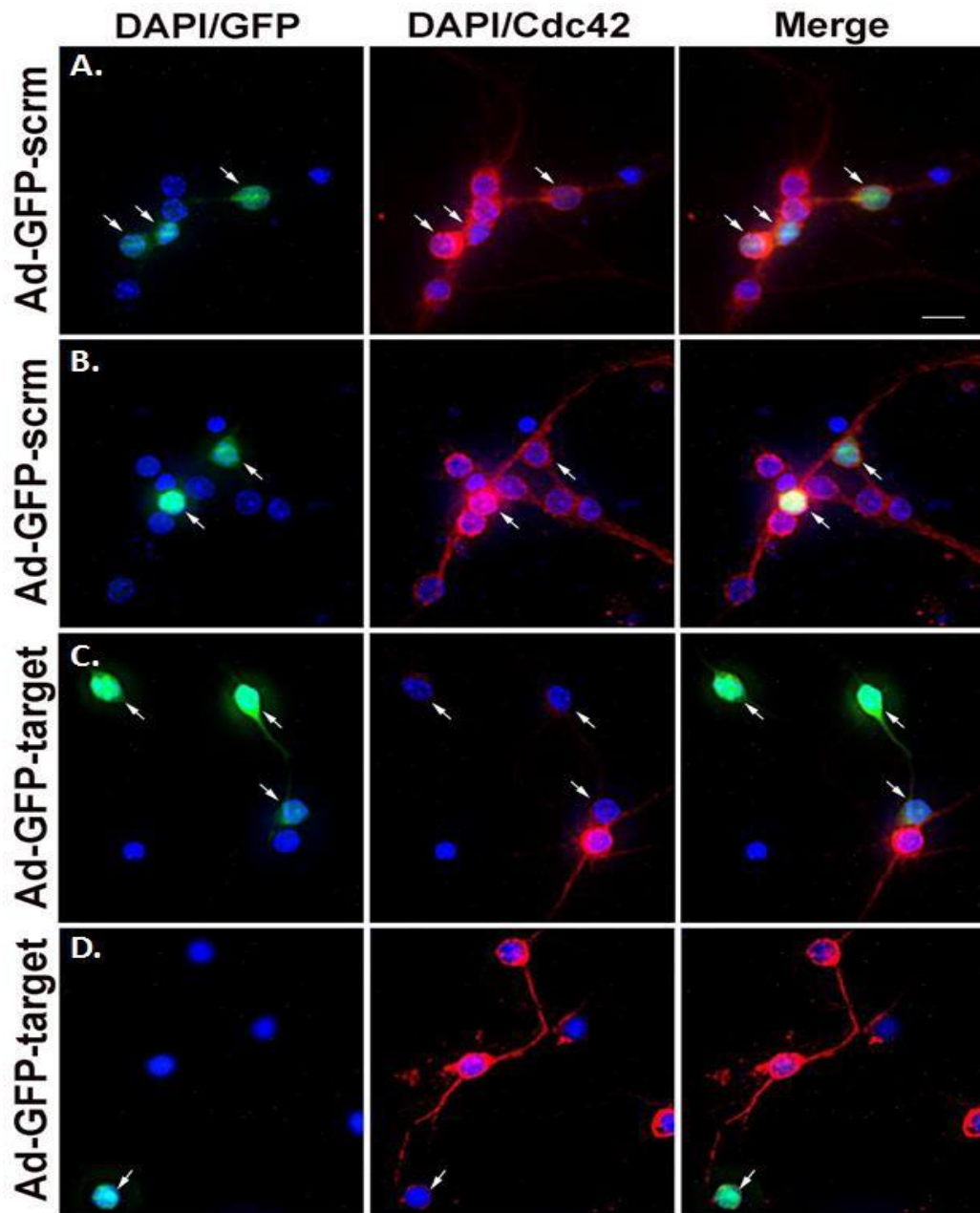
Figure 24: Immunocytochemistry for Cdc42 after 48 hour adenoviral infection. Representative micrographs of CGNs in 25K+ media after a 48 hour infection period with adenoviral shRNA constructs co-expressing GFP. From left to right, panels show virally infected cells (DAPI/GFP), Cdc42 content within cells (DAPI/Cdc42), and a merge of both images. Blue fluorescence indicates nuclei. Green fluorescence indicates positive GFP expression and viral infection. Red fluorescence indicates Cdc42. White arrows indicate virally infected cells. **A-B.** CGNs infected with scrambled (scrm) shRNA. **C-D.** CGNs infected with target Cdc42 shRNA. Note the lack of red fluorescence in GFP-expressing cells. Scale = 10 µm.
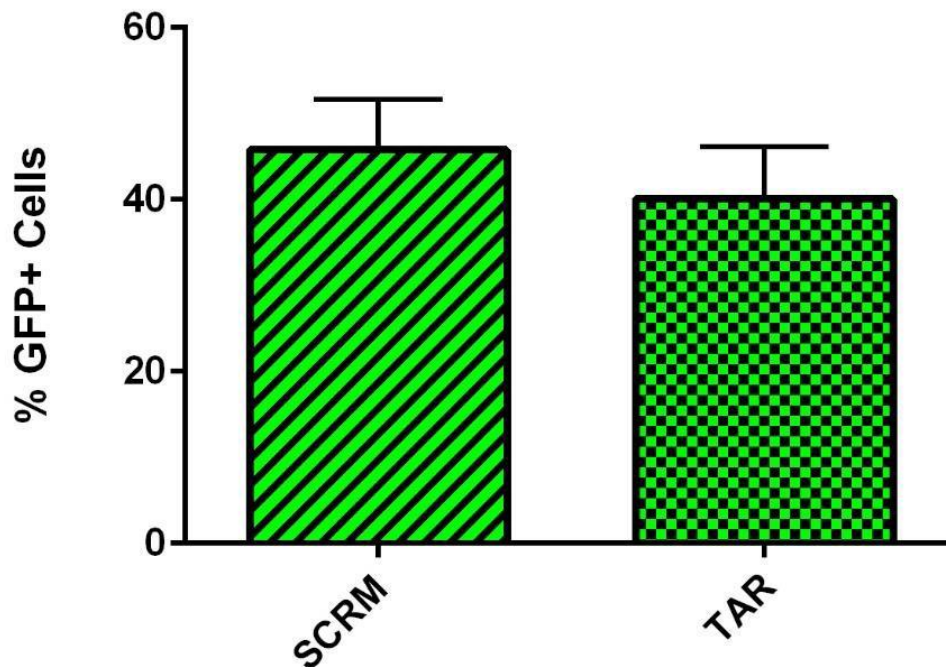
Figure 25: Quantification of GFP-positive CGNs after 72-hour adenoviral infection. Quantitative assessment of CGNs infected with GFP co-expressing, adenoviral constructs of either scrambled (SCRM) or Cdc42 target (TAR) shRNA. Approximately 200 GFP-expressing CGNs were quantified in duplicate wells per treatment for 3 experiments, and a percentage of GFP expressing cells was calculated for this group. There was no significant difference in the percentage of GFP-positive cells quantified between the scrambled and target conditions. Data were analyzed using an unpaired t-test, and are represented as the mean ± SEM, n=3.

Approximately 46% of the CGNs exposed to the scrambled shRNA and 40% of those exposed to the target shRNA became infected and were able to be quantified (Figure 25). With a Cdc42 knockdown efficiency of about 80% (as reported by Vector Biolabs), and around 40% of CGNs becoming infected with target shRNA in our experiments, we were able to achieve approximately 32% reduction of overall Cdc42 expression in our cell system. It is clear from Figure 26 that, not only was the target

71

shRNA effective at reducing the amount of Cdc42 (compare panels A-B to C-D), but also

that in the presence of 5K- stressful media, CGNs were sensitized to apoptotic cell death.

Quantification of these findings is represented in Figure 27, where it is shown that CGNs

infected with scrambled shRNA and exposed to 5K- media experienced an approximate

20 fold increase in apoptosis, and those infected with target Cdc42 shRNA an

approximate 80 fold increase in apoptosis. Overall there was a 4 fold increase in cell

death seen with the genetic inhibition of Cdc42 function, suggesting that Cdc42 does

possess some neuroprotective qualities in cells that are experiencing duress.
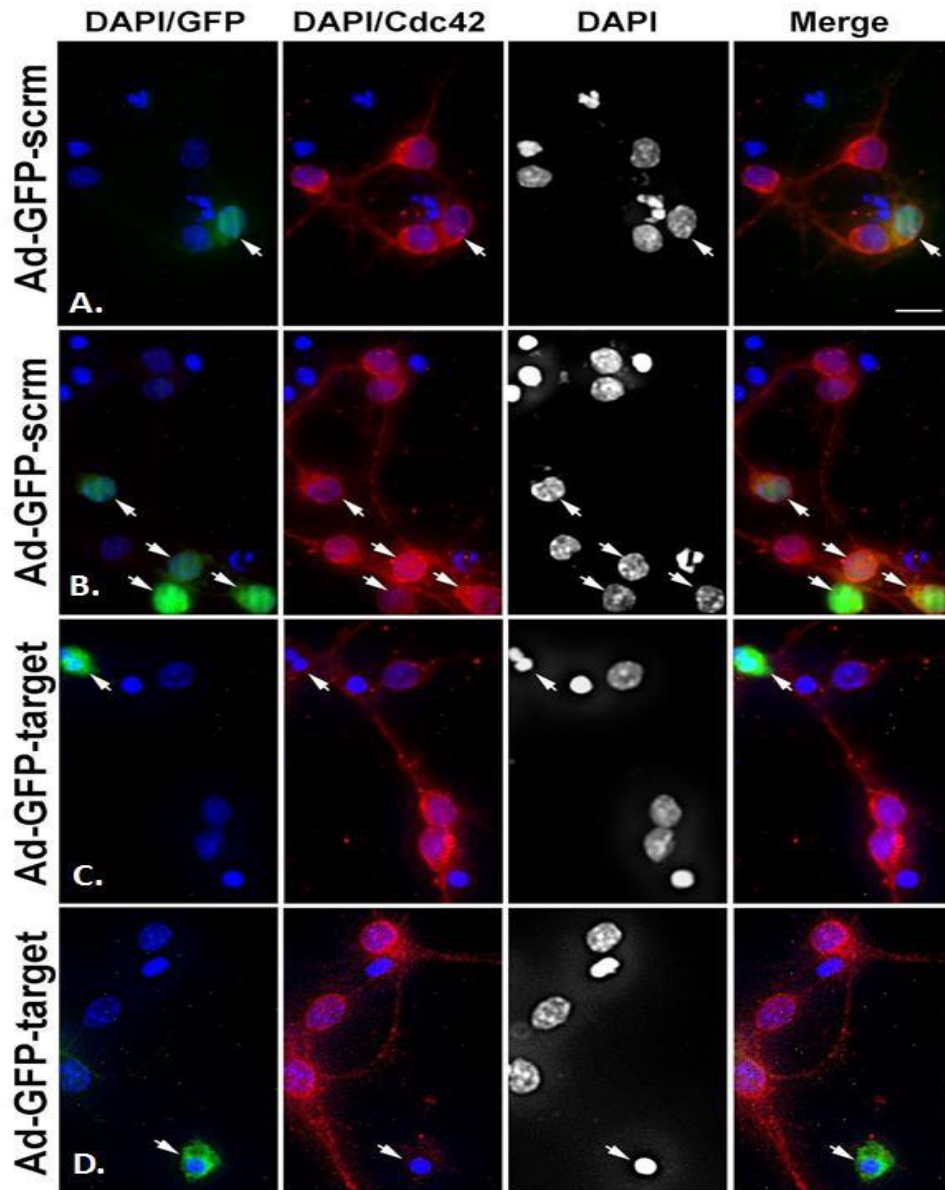
Figure 26: Immunocytochemistry for Cdc42 after 72 hour adenoviral knockdown and a 5K- media exchange. Representative micrographs of CGNs that were incubated in 25K+ media for an initial 48 hour infection period with adenoviral scrambled (scrm) or Cdc42 targeting shRNA constructs co-expressing GFP, and then underwent a 5K- media exposure for 24 hours. From left to right, panels show virally infected cells (DAPI/GFP), Cdc42 content within cells (DAPI/Cdc42), decolorized Hoechst staining alone (DAPI) and a merged image. Blue fluorescence indicates Hoechst staining. Green fluorescence indicates positive GFP expression and viral infection. Red fluorescence indicates Cdc42. White arrows designate virally infected cells. **A-B.** CGNs infected with scrambled (scrm) shRNA. **C-D.** CGNs infected with target Cdc42 shRNA. Scale = 10 µm. Note the lack of red fluorescence in cells expressing GFP.

73
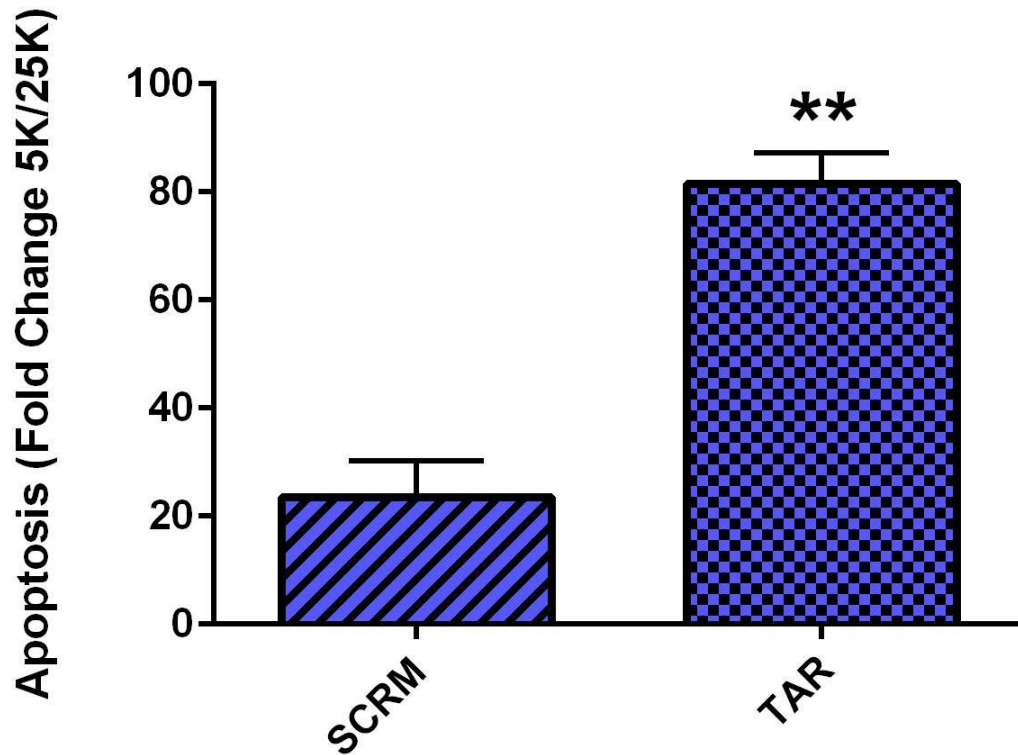
Figure 27: Quantification of apoptosis in CGNs after 72-hour adenoviral shRNA infection and a 5K- media exchange. Quantitative assessment of apoptosis (expressed as a fold change of 5K-/25K+) in CGNs after a 72-hour adenoviral infection with either scrambled (SCRM) or target Cdc42 (TAR) shRNA, and 24 hour exposure to 5K- media. 5K- media alone caused an approximate 20 fold increase in apoptosis, and target Cdc42 shRNA caused an approximate 80 fold increase in apoptosis. Data were analyzed using an unpaired t-test, and are represented as the mean ± SEM, n=3. ** indicates p<0.01 compared to scrambled shRNA infection in 5K- media.

Chapter Four: Discussion

Considering all of their responsibilities in biological functions such as regulation of the actin cytoskeleton, transcription factors, cell cycle progression, etc., it is not surprising that new roles for the Rho GTPase family as regulators of neuronal survival and apoptosis have emerged. Preceding research has strongly established a pro-survival role for Rac, and a pro-apoptotic role for Rho in neurons, and the effects of dysregulated Rho GTPase family members have started to become recognized pathological culprits in a variety of diseases. Cdc42, the least extensively investigated member of this family, is most well-known for its relationship with cancer and the survival of transformed cells, but to date, it has been relatively overlooked in terms of a contribution to neuronal survival and apoptosis.

Prior studies utilizing dominant negative mutants and *Clostridial* toxins to knockout the function of Cdc42 were performed under healthy growth conditions, and demonstrated a lack of necessity for Cdc42 for survival (Le et al. 2005). These studies show that inhibition of Rac activity, regardless of neuronal environment, will cause subsequent cell death. However, inhibition of Cdc42 alone did not significantly increase apoptosis, although both Rac and Cdc42 share many common target proteins, and have demonstrated similar biological function (i.e., neurite extension). Our study also confirmed the findings of that study, as our adenoviral shRNA obstruction of Cdc42 function in 25K+ media did not significantly increase cell death. While these studies

have adequately conveyed that Cdc42 is not absolutely essential to neuronal survival under normalized conditions, the role of Cdc42 in neuronal survival under arduous growth conditions, such as those that neurons experience during the progression of neurodegenerative disease, has not to our knowledge yet been explored. Our goal was to determine whether or not Cdc42 augments the survival of cerebellar granule neurons when they are already enduring stress.

Initial experiments show that chemical inhibition either broadly of Cdc42 function, or the function of its downstream effectors PAK and ACK-1, did convey additional apoptotic sensitivity to neurons experiencing withdrawal of both growth factor serum and depolarizing potassium (5K-). However, because PAK is also a known target of Rac, which is presently understood to be essential for neuronal survival, we chose not to heavily concentrate on it. In narrowing our focus to the two effectors solely targeted by Cdc42, ACK-1 and N-WASp, we discovered that chemical inhibition of N-WASp did not appear to significantly sensitize neurons to apoptosis under stressful growth conditions (Figures 18 and 19), so we did not further pursue a role for the Cdc42-N-WASp pathway in neuronal survival. From these experiment results, we determined that the Cdc42-ACK-1 and Cdc42-PAK signaling pathways do likely contribute to neuronal survival in some capacity. Also, based on our results using 187-1 and Wiskostatin inhibitosr, is conceivable that the N-WASp pathway contributes mainly, if not entirely, to actin cytoskeleton regulatory activities, and does not significantly take part in survival related tasks.

Chemical inhibition is a useful preliminary measure of protein function, however inhibitors often also have many off-target effects, which could potentially contribute to

any experimental results we observed. To rule out this possibility, we chose to use inhibitors with very dissimilar molecular structures (see Figures 8, 12, 15 and 17). Because the data were consistent within all of the particular inhibitor groups (i.e., all of the Cdc42 inhibitors increased apoptosis, but none of the N-WASp inhibitors did), it is highly unlikely that the survival effects we observed were due to off-target effects, rather than inhibition of the protein of interest. Also, we confirmed that our chemical inhibitors were efficacious in blocking their respective proteins with the use of both a G-LISA and Western blotting techniques. Cdc42 inhibitors ZCL278, Casin and ML141 were able to reduce the amount of active Cdc42 in our 5K- treatment samples, and both ZCL278 and AIM100 appeared to lower the amount of phosphorylated ACK-1, suggesting that this is how these inhibitors block ACK-1 activation.

While nuclear fragmentation and condensation are generally good indicators that apoptosis is transpiring, we wanted to confirm that it was what we were observing in our samples by both measuring metabolic activity and caspase release. Mitochondrial function was measured with the use of MTT assays, and we used immunocytochemistry techniques to explore the amount of caspase-3 release in our CGN samples. Figure 22 shows the dramatic reduction in mitochondrial function we observed after inhibition of Cdc42 and ACK-1 in 5K- media, indicating that blocking the activity of either protein significantly sensitized the neurons to cell death under stress. Also, Figure 23 shows that there was substantially more active caspase-3 released in CGN samples with inhibited Cdc42 or ACK-1 only under stressful conditions, and that there was little to none released in healthy, 25K+ culture media. These measures both confirm that the changes we observed in nuclear morphology were due to cell death.

77

To more definitely test any survival-related responsibilities of Cdc42 in strained CGNs, we used a genetic approach to block the production of Cdc42 protein, as opposed to just inhibiting its activity. Our adenoviral Cdc42 shRNA construct was able to successfully reduce Cdc42 levels by approximately 32% overall, and caused a 4 fold increase in cell death when cells were incubated with the virus in 5K- media. Also worth noting is the general lack of Cdc42 staining observed in apoptotic cells, regardless of treatment or shRNA viral infection (Figures 24 and 26). It is possible that this is a consequence of general Cdc42 degradation during apoptotic cell death, as Cdc42 has been previously shown to possess a caspase cleavage sensitivity consensus sequence (DXXD) near the Rho insert region (Tu and Cerione, 2001). These results more conclusively confirm that while Cdc42 function may not be an essential component to neuronal survival, it appears to convey some amount of neuroprotection to cells that are enduring stressful conditions. Collectively, our data suggest that Cdc42 is not absolutely necessary for neuronal survival as is Rac, but it likely is an additional pro-survival protein that contributes to neuronal survival during cellular duress. As neurons are progressively exposed to increasing levels of stress during the course of neurodegenerative diseases, Cdc42 could present as a potential therapeutic target in delaying disease advancement.

Chapter Five: Conclusions and Future Directions

Our *in vitro* experiments have provided evidence for the role of small Rho GTPase family member Cdc42 in neuronal survival. While studies have consistently shown that Cdc42 is not absolutely vital for neuronal survival, as is its sibling Rac, we wanted to determine whether it had any neuroprotective function at all. We induced cell death by removing both growth factor-containing serum and depolarizing potassium to model a stressful neuronal environment, and then manipulated the function either broadly of Cdc42, or of one of its downstream effectors (ACK-1, PAK or N-WASp). Through these studies, we were able to re-confirm that Cdc42 inhibition under healthy growth conditions did not impede neuronal survival, but that its inhibition, or that of its downstream effectors ACK-1 and PAK, did significantly sensitize neurons further to cell death. N-WASp inhibition did not appear to have any impact on neuronal survival. Our findings advocate a neuroprotective role for Cdc42 under strenuous neuronal environmental conditions, and suggest that it could be a viable therapeutic target in progressive neurodegenerative disease.

For future studies, we intend to perform similar experiments, but utilizing a different substance for the initial induction of cell death known as HA-14. HA-14 induces apoptosis by directly antagonizing pro-survival members of the Bcl-2 family (Bcl-w and Bcl-XL), as well as by disrupting the anti-apoptotic association between Bax and Bcl-2 (Chen et al. 2002). Stankiewicz et al. (2015) demonstrated how a Rac1 chemical inhibitor

known as NSC induced apoptotic cell death in CGNs by causing an increase in

mitochondrial localization and activation of pro-apoptotic Bcl-2 protein Bad. Many of the

survival pathways involved in Cdc42 signaling also impact Bcl-2 proteins (i.e.

PI3K/Akt), so if our results were similar with the use of HA-14, we could begin to define

more clearly the death mechanisms involved in Cdc42 inhibition. In addition, we would

like to conduct a Western blot panel for various BH-3 only proteins (i.e., Bim, Noxa,

Puma, Bad, etc.) after treatment of CGNs with ZCL278 and AIM100 in both 25K+ and

5K- media conditions. This could also indicate more precisely which death pathway is

occurring in our experiments. Also, we aim to more clearly ascertain the role of the

ACK-1 signaling pathway in neuronal survival, as its connection to survival in other cell

types has been well documented. We will obtain a constitutively active ACK-1 mutant

and see if survival can be rescued after treatment with a Cdc42 or ACK-1 specific

chemical inhibitor (i.e., ZCL278, AIM100) in stressful growth media.

We would also like to explore the role of Cdc42 in brain cancer, by manipulating

its function in human glioblastoma cell line U-87 MG. The current form of treatment

most commonly administered to glioblastoma multiforme (GBM) patients is an oral

chemotherapeutic agent called temozolomide (TMZ). TMZ is an alkylating agent that

works by methylating and damaging DNA in an attempt to destroy tumor cells, however

GBM is particularly evasive to treatment in general, and TMZ tends to only increase

lifespan by a few months without improvement in patient life quality (Stupp et al. 2005).

A study by Milano et al. (2009) detailed the use of Dasatinib as a potential therapeutic

agent to be used in combination with TMZ. Their study found that the co-treatment of

glioblastoma cells with Dasatinib and TMZ both increased autophagic cell death, and increased the efficacy of TMZ overall. However this study concluded that the results were due to Dasatinib's inhibition of Src kinases. Due to its multi-target impacts, we speculated that their results could have actually been an ACK-1 inhibitory consequence, as Dasatinib is also an ACK-1 inhibitor. We would like to use both AIM100 and ZCL278 in combination with TMZ to see if there is an impact on glioblastoma cell survival. As AIM100 is much more specific to ACK-1, if we achieve similar results, it is possible that the sensitization of cancer cells to TMZ is actually due to the inhibition of ACK-1 activity. Through these experiments, we hope to find that manipulation of Cdc42 could be an option in the treatment of other disease types.

References

Ahnert‑ Hilger, G., Höltje, M., Grosse, G., Pickert, G., Mucke, C., Nixdorf‑ Bergweiler, B., Boquet, P., Hofmann, F. & Just, I. (2004). Differential effects of Rho GTPases on axonal and dendritic development in hippocampal neurones. *Journal of neurochemistry*, *90*(1), 9-18.

Beal, M. F. (1998). Mitochondrial dysfunction in neurodegenerative diseases. *Biochimica et Biophysica Acta (BBA)-Bioenergetics*, *1366*(1), 211-223.

Biro, M., Munoz, M. A., & Weninger, W. (2014). Targeting Rho‑ GTPases in immune cell migration and inflammation. *British journal of pharmacology*, *171*(24), 5491-5506.

Boettner, B., & Van Aelst, L. (2002). The role of Rho GTPases in disease development. *Gene*, *286*(2), 155-174.

Bokoch, G. M. (2003). Biology of the p21-activated kinases. *Annual review of biochemistry*, *72*(1), 743-781.

Bressenot, A., Marchal, S., Bezdetnaya, L., Garrier, J., Guillemin, F., & Plénat, F. (2009). Assessment of apoptosis by immunohistochemistry to active caspase-3, active caspase-7, or cleaved PARP in monolayer cells and spheroid and subcutaneous xenografts of human carcinoma. *Journal of Histochemistry & Cytochemistry*, *57*(4), 289-300.

Brown, R. C., Lockwood, A. H., & Sonawane, B. R. (2005). Neurodegenerative diseases: an overview of environmental risk factors. *Environmental health perspectives*, *113*(9), 1250.

Buchwald, G., Hostinova, E., Rudolph, M. G., Kraemer, A., Sickmann, A., Meyer, H. E., Scheffzek, K. & Wittinghofer, A. (2001). Conformational switch and role of phosphorylation in PAK activation. *Molecular and cellular biology*, *21*(15), 5179-5189.

Burbelo, P. D., Drechsel, D., & Hall, A. (1995). A conserved binding motif defines numerous candidate target proteins for both Cdc42 and Rac GTPases. *Journal of Biological Chemistry*, *270*(49), 29071-29074.

Carlier, M. F., Ducruix, A., & Pantaloni, D. (1999). Signalling to actin: the Cdc42-N-WASP-Arp2/3 connection. *Chemistry & biology*, *6*(9), R235-R240.

Chen, J., Freeman, A., Liu, J., Dai, Q., & Lee, R. M. (2002). The Apoptotic Effect of HA14-1, a Bcl-2-interacting Small Molecular Compound, Requires Bax

Translocation and Is   Enhanced by PK11195 1 Supported by the Huntsman Cancer Foundation, Howard Hughes Medical Institute Fellow to Faculty Transition Program at the University of Utah. 1. *Molecular cancer therapeutics*, *1*(12), 981-987.

Chen, X., Guo, C., & Kong, J. (2012). Oxidative stress in neurodegenerative diseases. *Neural regeneration research*, *7*(5), 376.

Chuang, T. H., Hahn, K. M., Lee, J. D., Danley, D. E., & Bokoch, G. M. (1997). The small GTPase Cdc42 initiates an apoptotic signaling pathway in Jurkat T lymphocytes. *Molecular biology of the cell*, *8*(9), 1687-1698.

Connolly, M., Veale, D. J., & Fearon, U. (2011). Acute serum amyloid A regulates cytoskeletal rearrangement, cell matrix interactions and promotes cell migration in rheumatoid arthritis. *Annals of the rheumatic diseases*, annrheumdis142240.

Côté, J. F., & Vuori, K. (2006). In Vitro Guanine Nucleotide Exchange Activity of DHR- 2/DOCKER/CZH2 Domains. *Methods in enzymology*, *406*, 41-57.

Datta, S. R., Dudek, H., Tao, X., Masters, S., Fu, H., Gotoh, Y., & Greenberg, M. E. (1997). Akt phosphorylation of BAD couples survival signals to the cell-intrinsic death machinery. *Cell*, *91*(2), 231-241.

DiMauro, E. F., Newcomb, J., Nunes, J. J., Bemis, J. E., Boucher, C., Buchanan, J. L., Buckner, W. H., Cheng, A., Faust, T., Hsieh, F., Huang, X., Lee, J. H., Marshall, T. L., Martin, M. W., McGowan, D. C., Schneider, S., Turci, S. M., White, R. D. & Zhu, X. (2007). Discovery of 4-amino-5, 6-biaryl-furo [2, 3-d] pyrimidines as inhibitors of Lck: development of an expedient and divergent synthetic route and preliminary SAR. *Bioorganic & medicinal chemistry letters*, *17*(8), 2305-2309.

D'Mello, S. R., Galli, C., Ciotti, T., & Calissano, P. (1993). Induction of apoptosis in cerebellar granule neurons by low potassium: inhibition of death by insulin-like growth factor I and cAMP. *Proceedings of the National Academy of Sciences*, *90*(23), 10989-10993.

Dolan, B. M., Duron, S. G., Campbell, D. A., Vollrath, B., Rao, B. S., Ko, H. Y., Lin, G. G., Govindarajan, A., Choi, S. Y. & Tonegawa, S. (2013). Rescue of fragile X syndrome phenotypes in Fmr1 KO mice by the small-molecule PAK inhibitor FRAX486. *Proceedings of the National Academy of Sciences*, *110*(14), 5671-5676.

Driver, J. A. (2014). Inverse association between cancer and neurodegenerative disease: review of the epidemiologic and biological evidence. *Biogerontology*, *15*(6), 547.

Dummler, B., Ohshiro, K., Kumar, R., & Field, J. (2009). Pak protein kinases and their role in cancer. *Cancer and Metastasis Reviews*, *28*(1), 51-63.

Duprez, L., Wirawan, E., Berghe, T. V., & Vandenabeele, P. (2009). Major cell death pathways at a glance. *Microbes and infection*, *11*(13), 1050-1062.

Edwards, D. C., & Gill, G. N. (1999). Structural features of LIM kinase that control effects on the actin cytoskeleton. *Journal of Biological Chemistry*, *274*(16), 11352-11361.

Etienne-Manneville, S. (2004). Cdc42-the centre of polarity. *Journal of cell science*, *117*(8), 1291- 1300.

Eustace, A. J., Crown, J., Clynes, M., & O'Donovan, N. (2008). Preclinical evaluation of dasatinib, a potent Src kinase inhibitor, in melanoma cell lines. *Journal of translational medicine*, *6*(1), 53.

Florian, M. C., Dörr, K., Niebel, A., Daria, D., Schrezenmeier, H., Rojewski, M., Filippi, M. D., Hasenberg, A., Gunzer, M., Scharffetter-Kochanek, K., Zheng, Y. & Geiger, H. (2012). Cdc42 activity regulates hematopoietic stem cell aging and rejuvenation. *Cell stem cell*, *10*(5), 520-530.

Fournier, A. E., Takizawa, B. T., & Strittmatter, S. M. (2003). Rho kinase inhibition enhances axonal regeneration in the injured CNS. *Journal of Neuroscience*, *23*(4) , 1416-1423.

Foster, I. (2008). Cancer: A cell cycle defect. *Radiography*, *14*(2), 144-149.

Fried, S., Matalon, O., Noy, E., & Barda-Saad, M. (2014). WIP: more than a WASp-interacting protein. *Journal of leukocyte biology*, *96*(5), 713-727.

Friesland, A., Zhao, Y., Chen, Y. H., Wang, L., Zhou, H., & Lu, Q. (2013). Small molecule targeting Cdc42–intersectin interaction disrupts Golgi organization and suppresses cell motility. *Proceedings of the National Academy of Sciences*, *110*(4), 1261-1266.

Frugtniet, B. A., Martin, T. A., Zhang, L., & Jiang, W. G. (2017). Neural Wiskott-Aldrich syndrome protein (nWASP) is implicated in human lung cancer invasion. *BMC cancer*, *17*(1), 224.

Galli, C., Meucci, O., Scorziello, A., Werge, T. M., Calissano, P., & Schettini, G. (1995). Apoptosis in cerebellar granule cells is blocked by high KCl, forskolin, and IGF-1 through distinct mechanisms of action: the involvement of intracellular calcium and RNA synthesis. *Journal of Neuroscience*, *15*(2), 1172-1179.

Ginham, R., Harrison, D. C., Facci, L., Skaper, S., & Philpott, K. L. (2001). Upregulation of death pathway molecules in rat cerebellar granule neurons undergoing apoptosis. *Neuroscience letters*, *302*(2), 113-116.

Govek, E. E., Newey, S. E., & Van Aelst, L. (2005). The role of the Rho GTPases in neuronal development. *Genes & development*, *19*(1), 1-49.

Guerriero, C. J., & Weisz, O. A. (2007). N-WASP inhibitor wiskostatin nonselectively perturbs membrane transport by decreasing cellular ATP levels. *American Journal of Physiology-Cell Physiology*, *292*(4), C1562-C1566.

Guo, F., & Zheng, Y. (2004). Involvement of Rho family GTPases in p19Arf-and p53-mediated proliferation of primary mouse embryonic fibroblasts. *Molecular and cellular biology*, *24*(3), 1426-1438.

Gupton, S. L., & Gertler, F. B. (2007). Filopodia: the fingers that do the walking. *Science Signaling*, *2007*(400), re5.

Hadano, S., Kunita, R., Otomo, A., Suzuki-Utsunomiya, K., & Ikeda, J. E. (2007). Molecular and cellular function of ALS2/alsin: implication of membrane dynamics in neuronal development and degeneration. *Neurochemistry international*, *51*(2), 74-84.

Hakoshima, T., Shimizu, T., & Maesaki, R. (2003). Structural basis of the Rho GTPase signaling. *Journal of biochemistry*, *134*(3), 327-331.

Hall, A. (2005). Rho GTPases and the control of cell behaviour. *Biochemical Society Transactions*, *33*(5), 891-895.

Hanna, S., & El-Sibai, M. (2013). Signaling networks of Rho GTPases in cell motility. *Cellular signalling*, *25*(10), 1955-1961.

Hayashi-Takagi, A., Araki, Y., Nakamura, M., Vollrath, B., Duron, S. G., Yan, Z., Kasai, H., Huganir, R. L., Campbell, D. & Sawa, A. (2014). PAKs inhibitors ameliorate schizophrenia-associated dendritic spine deterioration in vitro and in vivo during late adolescence. *Proceedings of the National Academy of Sciences*, *111*(17), 6461-6466.

Higgs, H. N., & Pollard, T. D. (1999). Regulation of actin polymerization by Arp2/3 complex and WASp/Scar proteins. *Journal of Biological Chemistry*, *274*(46), 32531-32534.

Hoffman, G. R., & Cerione, R. A. (2000). Flipping the switch: minireview the structural basis for signaling through the CRIB motif. *Cell*, *102*(4), 403-406.

Hofmann, J., Sommer, M., Jarosch, E., Lenk, U., & Hein, L. (2000). *Reviews of physiology, biochemistry and pharmacology* (Vol. 142). Springer Science & Business Media.

Holbert, S., Dedeoglu, A., Humbert, S., Saudou, F., Ferrante, R. J., & Néri, C. (2003). Cdc42-interacting protein 4 binds to huntingtin: neuropathologic and biological evidence for a role in Huntington's disease. *Proceedings of the National Academy of Sciences*, *100*(5), 2712-2717.

Hong, L., Kenney, S. R., Phillips, G. K., Simpson, D., Schroeder, C. E., Nöth, J., Romero, E., Swanson, S., Waller A., Strouse, J. J., Carter, M., Chigaev, A., Ursu, O., Oprea, T., Hjelle, B., Golden, J. E., Aubé, J., Hudson, L. G., Buranda, T., Sklar, L. A. & Wandinger-Ness, A. (2013). Characterization of a Cdc42 protein inhibitor and its use as a molecular probe. *Journal of Biological Chemistry*, *288*(12), 8531-8543.

Ip, C. K. M., Cheung, A. N. Y., Ngan, H. Y. S., & Wong, A. S. T. (2011). p70 S6 kinase in the control of actin cytoskeleton dynamics and directed migration of ovarian cancer cells. *Oncogene*, *30*(21), 2420-2432.

Itakura, A., Aslan, J. E., Kusanto, B. T., Phillips, K. G., Porter, J. E., Newton, P. K., Nan, X., Insall, R. H., Chernoff, J. & McCarty, O. J. (2013). p21-Activated kinase (PAK) regulates cytoskeletal reorganization and directional migration in human neutrophils. *PloS one*, *8*(9), e73063.

Jin, Z., & Strittmatter, S. M. (1997). Rac1 mediates collapsin-1-induced growth cone collapse. *Journal of Neuroscience*, *17*(16), 6256-6263.

Kim, A. S., Kakalis, L. T., Abdul-Manan, N., Liu, G. A., & Rosen, M. K. (2000). Autoinhibition and activation mechanisms of the Wiskott–Aldrich syndrome protein. *Nature*, *404*(6774), 151-158.

Kirchhausen, T., & Rosen, F. S. (1996). Disease mechanism: unravelling Wiskott–Aldrich syndrome. *Current Biology*, *6*(6), 676-678.

Kranenburg, O., Poland, M., van Horck, F. P., Drechsel, D., Hall, A., & Moolenaar, W. H. (1999). Activation of RhoA by lysophosphatidic acid and Gα12/13 subunits in neuronal cells: induction of neurite retraction. *Molecular biology of the cell*, *10*(6), 1851-1857.

Krysko, D. V., Kaczmarek, A., & Vandenabeele, P. (2009). Molecular Pathways of Different Types of Cell Death: Many Roads to Death. In *Phagocytosis of Dying Cells: From Molecular Mechanisms to Human Diseases* (pp. 3-31). Springer Netherlands.

Kubo, T., Yamashita, T., Yamaguchi, A., Sumimoto, H., Hosokawa, K., & Tohyama, M. (2002). A novel FERM domain including guanine nucleotide exchange factor is involved in Rac signaling and regulates neurite remodeling. *Journal of Neuroscience*, *22*(19), 8504-8513.

La Torre, A., del Rio, J. A., Soriano, E., & Ureña, J. M. (2006). Expression pattern of ACK1 tyrosine kinase during brain development in the mouse. *Gene expression patterns*, *6*(8), 886-892.

Lai, T. W., Zhang, S., & Wang, Y. T. (2014). Excitotoxicity and stroke: identifying novel targets for neuroprotection. *Progress in neurobiology*, *115*, 157-188.

Le, S. S., Loucks, F. A., Udo, H., Richardson‐Burns, S., Phelps, R. A., Bouchard, R. J., Barth, H., Aktories, K., Tyler, K. L., Kandel, E. R., Heidenreich, K. A. & Linseman, D. A. (2005). Inhibition of Rac GTPase triggers ac‐Jun‐ and Bim‐dependent mitochondrial apoptotic cascade in cerebellar granule neurons. *Journal of neurochemistry*, *94*(4), 1025-1039.

Legg, J. A., Bompard, G., Dawson, J., Morris, H. L., Andrew, N., Cooper, L., Johnston, S. A., Tramountanis, G. & Machesky, L. M. (2007). N-WASP involvement in dorsal ruffle formation in mouse embryonic fibroblasts. *Molecular biology of the cell*, *18*(2), 678-687.

Lei, M., Lu, W., Meng, W., Parrini, M. C., Eck, M. J., Mayer, B. J., & Harrison, S. C. (2000). Structure of PAK1 in an autoinhibited conformation reveals a multistage activation switch. *Cell*, *102*(3), 387-397.

Li, J., Rix, U., Fang, B., Bai, Y., Edwards, A., Colinge, J., Bennett, K. L., Gao, J., Song, L., Eschrich, S., Superti-Furga, G., Koomen, J. & Haura, E. B. (2010). A chemical and phosphoproteomic characterization of dasatinib action in lung cancer. *Nature chemical biology*, *6*(4), 291-299.

Lin, R., Bagrodia, S., Cerione, R., & Manor, D. (1997). A novel Cdc42Hs mutant induces cellular transformation. *Current Biology*, *7*(10), 794-797.

Linseman, D. A., Heidenreich, K. A., & Fisher, S. K. (2001). Stimulation of M3 muscarinic receptors induces phosphorylation of the Cdc42 effector activated Cdc42Hs-associated kinase-1 via a Fyn tyrosine kinase signaling pathway. *Journal of Biological Chemistry*, *276*(8), 5622-5628.

Linseman, D. A., Laessig, T., Meintzer, M. K., McClure, M., Barth, H., Aktories, K., & Heidenreich, K. A. (2001). An essential role for Rac/Cdc42 GTPases in cerebellar granule neuron survival. *Journal of Biological Chemistry*, *276*(42), 39123-39131.

Linseman, D. A., & Loucks, F. A. (2008). Diverse roles of Rho family GTPases in neuronal development, survival, and death. *Frontiers in bioscience: a journal and virtual library*, *13*, 657-676.

Lombardo, L. J., Lee, F. Y., Chen, P., Norris, D., Barrish, J. C., Behnia, K., Castaneda, S., Cornelius, L. A. M., Das, J., Doweyko, A. M., Fairchild, C., Hunt, J. T., Inigo, I., Johnston, K., Kamath, A., Kan, D., Klei, H., Marathe, P., Pang, S., Peterson, R., Pitt, S., Schieven, G. L., Schmidt, R. J., Tokarski, J., Wen, M. L., Wityak, J. & Borzilleri, R. M. (2004). Discovery of N-(2-chloro-6-methyl-phenyl)-2-(6-(4-(2-hydroxyethyl)-piperazin-1-yl)-2-methylpyrimidin-4-ylamino) thiazole-5-carboxamide (BMS-354825), a dual Src/Abl kinase inhibitor with potent antitumor activity in preclinical assays. *Journal of medicinal chemistry*, *47*(27), 6658-6661.

Loucks, F. A., Le, S. S., Zimmermann, A. K., Ryan, K. R., Barth, H., Aktories, K., & Linseman, D. A. (2006). Rho family GTPase inhibition reveals opposing effects of mitogen‐activated protein kinase kinase/extracellular signal‐regulated kinase and Janus kinase/signal transducer and activator of transcription signaling cascades on neuronal survival. *Journal of neurochemistry*, *97*(4), 957-967.

Lougheed, J. C., Chen, R. H., Mak, P., & Stout, T. J. (2004). Crystal structures of the phosphorylated and unphosphorylated kinase domains of the Cdc42-associated tyrosine kinase ACK1. *Journal of Biological Chemistry*, *279*(42), 44039-44045.

Lundquist, E. A. (2003). Rac proteins and the control of axon development. *Current opinion in neurobiology*, *13*(3), 384-390.

Luo, L. (2000). Rho GTPases in neuronal morphogenesis. *Nature Reviews Neuroscience*, *1*(3),173-180.

Ma, Q. L., Yang, F., Frautschy, S. A., & Cole, G. M. (2012). PAK in Alzheimer disease, Huntington disease and X-linked mental retardation. *Cellular logistics*, *2*(2), 117-125.

Mahajan, K., Challa, S., Coppola, D., Lawrence, H., Luo, Y., Gevariya, H., Zhu, W., Chen, Y. A., Lawrence, N. J. & Mahajan, N. P. (2010). Effect of Ack1 tyrosine kinase inhibitor on ligand‐independent androgen receptor activity. *The Prostate*, *70*(12), 1274-1285.

Mahajan, K., Coppola, D., Chen, Y. A., Zhu, W., Lawrence, H. R., Lawrence, N. J., & Mahajan, N. P. (2012). Ack1 tyrosine kinase activation correlates with pancreatic cancer progression. *The American journal of pathology*, *180*(4), 1386-1393.

Mahajan, N. P., Liu, Y., Majumder, S., Warren, M. R., Parker, C. E., Mohler, J. L., Earp, H. S. & Whang, Y. E. (2007). Activated Cdc42-associated kinase Ack1 promotes prostate cancer progression via androgen receptor tyrosine phosphorylation. *Proceedings of the National Academy of Sciences*, *104*(20), 8438-8443.

Mahajan, K., & Mahajan, N. P. (2013). ACK1 tyrosine kinase: targeted inhibition to block cancer cell proliferation. *Cancer letters*, *338*(2), 185-192.

Mahajan, K., & Mahajan, N. P. (2015). ACK1/TNK2 tyrosine kinase: molecular signaling and evolving role in cancers. *Oncogene*, *34*(32), 4162-4167.

Mahajan, K., & Mahajan, N. P. (2010). Shepherding AKT and androgen receptor by Ack1 tyrosine kinase. *Journal of cellular physiology*, *224*(2), 327-333.

Mahajan, N. P., Whang, Y. E., Mohler, J. L., & Earp, H. S. (2005). Activated tyrosine kinase Ack1 promotes prostate tumorigenesis: role of Ack1 in polyubiquitination of tumor suppressor Wwox. *Cancer research*, *65*(22), 10514-10523.

Martin, L. J., Al-Abdulla, N. A., Brambrink, A. M., Kirsch, J. R., Sieber, F. E., & Portera-Cailliau, C. (1998). Neurodegeneration in excitotoxicity, global cerebral ischemia, and target deprivation: a perspective on the contributions of apoptosis and necrosis. *Brain research bulletin*, *46*(4), 281-309.

Melendez, J., Grogg, M., & Zheng, Y. (2011). Signaling role of Cdc42 in regulating mammalian physiology. *Journal of Biological Chemistry*, *286*(4), 2375-2381.

Meller, N., Irani-Tehrani, M., Kiosses, W. B., Del Pozo, M. A., & Schwartz, M. A. (2002). Zizimin1, a novel Cdc42 activator, reveals a new GEF domain for Rho proteins. *Nature cell biology*, *4*(9), 639-647.

Milano, V., Piao, Y., LaFortune, T., & de Groot, J. (2009). Dasatinib-induced autophagy is enhanced in combination with temozolomide in glioma. *Molecular cancer therapeutics*, *8*(2), 394-406.

Modzelewska, K., Newman, L. P., Desai, R., & Keely, P. J. (2006). Ack1 mediates Cdc42-dependent cell migration and signaling to p130Cas. *Journal of Biological Chemistry*, *281*(49), 37527-37535.

Munemitsu, S., Innis, M. A., Clark, R., McCormick, F., Ullrich, A., & Polakis, P. (1990). Molecular cloning and expression of a G25K cDNA, the human homolog of the yeast cell cycle gene CDC42. *Molecular and cellular biology*, *10*(11), 5977-5982.

Nobes, C. D., & Hall, A. (1999). Rho GTPases control polarity, protrusion, and adhesion during cell movement. *The Journal of cell biology*, *144*(6), 1235-1244.

O'Keefe, E. P. (2013). siRNAs and shRNAs: Tools for protein knockdown by gene silencing. *Word Lab*.

Olenik, C., Barth, H., Just, I., Aktories, K., & Meyer, D. K. (1997). Gene expression of the small GTP-binding proteins RhoA, RhoB, Rac1, and Cdc42 in adult rat brain. *Molecular brain research*, *52*(2), 263-269.

Olson, M. F., Ashworth, A., & Hall, A. (1995). An essential role for Rho, Rac, and Cdc42 GTPases in cell cycle progression through G1. *SCIENCE-NEW YORK THEN WASHINGTON-*, 1270-1270.

Oppenheim, R. W. (1991). Cell death during development of the nervous system. *Annual review of neuroscience*, *14*(1), 453-501.

Peterson, J. R., Bickford, L. C., Morgan, D., Kim, A. S., Ouerfelli, O., Kirschner, M. W., & Rosen, M. K. (2004). Chemical inhibition of N-WASP by stabilization of a native autoinhibited conformation. *Nature structural & molecular biology*, *11*(8), 747-755.

Peterson, J. R., Lebensohn, A. M., Pelish, H. E., & Kirschner, M. W. (2006). Biochemical suppression of small-molecule inhibitors: a strategy to identify inhibitor targets and signaling pathway components. *Chemistry & biology*, *13*(4), 443-452.

Peterson, J. R., Lokey, R. S., Mitchison, T. J., & Kirschner, M. W. (2001). A chemical inhibitor of N-WASP reveals a new mechanism for targeting protein interactions. *Proceedings of the National Academy of Sciences*, *98*(19), 10624-10629.

Portt, L., Norman, G., Clapp, C., Greenwood, M., & Greenwood, M. T. (2011). Anti-apoptosis and cell survival: a review. *Biochimica et Biophysica Acta (BBA)-Molecular Cell Research*, *1813*(1), 238-259.

Prehoda, K. E., Scott, J. A., Mullins, R. D., & Lim, W. A. (2000). Integration of multiple signals through cooperative regulation of the N-WASP-Arp2/3 complex. *Science*, *290*(5492), 801-806.

Qiu, R. G., Abo, A., McCormick, F., & Symons, M. (1997). Cdc42 regulates anchorage-independent growth and is necessary for Ras transformation. *Molecular and cellular biology*, *17*(6), 3449-3458.

Radu, M., Semenova, G., Kosoff, R., & Chernoff, J. (2014). PAK signalling during the development and progression of cancer. *Nature reviews Cancer*, *14*(1), 13-25.

Resh, M. D. (2013). Covalent lipid modifications of proteins. *Current Biology*, *23*(10), R431-R435.

Riss, T. L., Moravec, R. A., Niles, A. L., Duellman, S., Benink, H. A., Worzella, T. J., & Minor, L. (2016). Cell viability assays.

Rohatgi, R., Ho, H. Y. H., & Kirschner, M. W. (2000). Mechanism of N-WASP activation by CDC42 and phosphatidylinositol 4, 5-bisphosphate. *The Journal of cell biology*, *150*(6), 1299-1310.

Rohatgi, R., Ma, L., Miki, H., Lopez, M., Kirchhausen, T., Takenawa, T., & Kirschner, M. W. (1999). The interaction between N-WASP and the Arp2/3 complex links Cdc42-dependent signals to actin assembly. *Cell*, *97*(2), 221-231.

Rosdahl, J. A., Ensslen, S. E., Niedenthal, J. A., & Brady‐Kalnay, S. M. (2003). PTPμ‐ dependent growth cone rearrangement is regulated by Cdc42. *Developmental Neurobiology*, *56*(3), 199-208.

Rossman, K. L., Der, C. J., & Sondek, J. (2005). GEF means go: turning on RHO GTPases with guanine nucleotide-exchange factors. *Nature reviews Molecular cell biology*, *6*(2), 167-180.

Schaefer, A., Reinhard, N. R., & Hordijk, P. L. (2014). Toward understanding RhoGTPase specificity: structure, function and local activation. *Small GTPases*, *5*(2), e968004.

Schoenherr, J. A., Drennan, J. M., Martinez, J. S., Chikka, M. R., Hall, M. C., Chang, H. C., & Clemens, J. C. (2012). Drosophila activated Cdc42 kinase has an anti-apoptotic function. *PLoS genetics*, *8*(5), e1002725.

Schmidt, A., & Hall, A. (2002). Guanine nucleotide exchange factors for Rho GTPases: turning on the switch. *Genes & development*, *16*(13), 1587-1609.

Shinjo, K., Koland, J. G., Hart, M. J., Narasimhan, V., Johnson, D. I., Evans, T., & Cerione, R. A. (1990). Molecular cloning of the gene for the human placental GTP-binding protein Gp (G25K): identification of this GTP-binding protein as the

human homolog of the yeast cell-division-cycle protein CDC42. *Proceedings of the National Academy of Sciences*, *87*(24), 9853-9857.

Sinha, S., & Yang, W. (2008). Cellular signaling for activation of Rho GTPase Cdc42. *Cellular signalling*, *20*(11), 1927-1934.

Stankiewicz, T. R., & Linseman, D. A. (2014). Rho family GTPases: key players in neuronal development, neuronal survival, and neurodegeneration. *Frontiers in cellular neuroscience*, *8*.

Stankiewicz, T. R., Loucks, F. A., Schroeder, E. K., Nevalainen, M. T., Tyler, K. L., Aktories, K., Bouchard, R. J. & Linseman, D. A. (2012). Signal transducer and activator of transcription-5 mediates neuronal apoptosis induced by inhibition of Rac GTPase activity. *Journal of Biological Chemistry*, *287*(20), 16835-16848

Stankiewicz, T. R., Ramaswami, S. A., Bouchard, R. J., Aktories, K., & Linseman, D. A. (2015). Neuronal apoptosis induced by selective inhibition of Rac GTPase versus global suppression of Rho family GTPases is mediated by alterations in distinct mitogen-activated protein kinase signaling cascades. *Journal of Biological Chemistry*, *290*(15), 9363-9376.

Stengel, K., & Zheng, Y. (2011). Cdc42 in oncogenic transformation, invasion, and tumorigenesis. *Cellular signalling*, *23*(9), 1415-1423.

Stupp, R., Mason, W. P., Van Den Bent, M. J., Weller, M., Fisher, B., Taphoorn, M. J., Belanger, K., Brandes, A. A., Marosi, C., Bogdahn, U., Curschmann, J., Janzer, R. C., Ludwin, S. K., Gorlia, T., Allgeier, A., Lacombe, D., Cairncross, G., Eisenhauer, E. & Mirimanoff, R. O. (2005). Radiotherapy plus concomitant and adjuvant temozolomide for glioblastoma. *New England Journal of Medicine*, *352*(10), 987-996.

Suetsugu, S., Hattori, M., Miki, H., Tezuka, T., Yamamoto, T., Mikoshiba, K., & Takenawa, T. (2002). Sustained activation of N-WASP through phosphorylation is essential for neurite extension. *Developmental cell*, *3*(5), 645-658.

Sumi, T., Matsumoto, K., Takai, Y., & Nakamura, T. (1999). Cofilin phosphorylation and actin cytoskeletal dynamics regulated by rho-and Cdc42-activated LIM-kinase 2. *The Journal of cell biology*, *147*(7), 1519-1532.

Surviladze, Z., Waller, A., Strouse, J. J., Bologa, C., Ursu, O., Salas, V., Parkinson, J. F., Phillips, G. K., Romero, E., Wandinger-Ness, A. & Sklar, L.A. (2010). A potent and selective inhibitor of Cdc42 GTPase.

Symons, M., & Settleman, J. (2000). Rho family GTPases: more than simple switches. *Trends in cell biology*, *10*(10), 415-419.

Tanaka, T., Tatsuno, I., Uchida, D., Moroo, I., Morio, H., Nakamura, S., Noguchi, Y., Yasuda, T., Kitagawa, M., Saito, Y. & Hirai, A. (2000). Geranylgeranyl-pyrophosphate, an isoprenoid of mevalonate cascade, is a critical compound for rat primary cultured cortical neurons to protect the cell death induced by 3-hydroxy-3-methylglutaryl-CoA reductase inhibition. *Journal of Neuroscience*, *20*(8), 2852-2859.

Taxman, D. J., Moore, C. B., Guthrie, E. H., & Huang, M. T. H. (2010). Short hairpin RNA (shRNA): design, delivery, and assessment of gene knockdown. *RNA Therapeutics: Function, Design, and Delivery*, 139-156.

Tu, S., & Cerione, R. A. (2001). Cdc42 is a substrate for caspases and influences Fas-induced apoptosis. *Journal of Biological Chemistry*, *276*(22), 19656-19663.

Ureña, J. M., La Torre, A., Martínez, A., Lowenstein, E., Franco, N., Winsky-Sommerer, R., Fontana, X., Casaroli-Marano, R., Ibáñez-Sabio, M. A., Pascual, M., Del Rio, J. A., de Lecea, L. & Soriano, E. (2005). Expression, synaptic localization, and developmental regulation of Ack1/Pyk1, a cytoplasmic tyrosine kinase highly expressed in the developing and adult brain. *Journal of Comparative Neurology*, *490*(2), 119-132.

Vakifahmetoglu, H., Olsson, M., & Zhivotovsky, B. (2008). Death through a tragedy: mitotic catastrophe. *Cell Death & Differentiation*, *15*(7), 1153-1162.

Valdés-Mora, F., Gómez, D. P. T., & Lacal, J. C. (2009). CDC42 (cell division cycle 42 (GTP binding protein, 25kDa)).

Västrik, I., Eickholt, B. J., Walsh, F. S., Ridley, A., & Doherty, P. (1999). Sema3A-induced growth-cone collapse is mediated by Rac1 amino acids 17–32. *Current biology*, *9*(18), 991-998.

Wells, C. M., & Jones, G. E. (2010). The emerging importance of group II PAKs. *Biochemical Journal*, *425*(3), 465-473.

Vega, F. M., & Ridley, A. J. (2008). Rho GTPases in cancer cell biology. *FEBS letters*, *582*(14), 2093-2101.

Volpi, S., Santori, E., Abernethy, K., Mizui, M., Dahlberg, C. I., Recher, M., Capuder, K., Csizmadia, E., Ryan, D., Mathew, D., Tsokos, G. C., Snapper, S., Westerberg, L. S., Thrasher, A. J., Candotti, F. & Notarangelo, L. D. (2016). N-WASP is

required for B-cell–mediated autoimmunity in Wiskott-Aldrich syndrome. *Blood*, *127*(2), 216-220.

Wang, Y., Gratzke, C., Tamalunas, A., Wiemer, N., Ciotkowska, A., Rutz, B., Waidelich, R., Strittmatter, F., Liu, C., Stief, C. G. & Hennenberg, M. (2016). P21-activated kinase inhibitors FRAX486 and IPA3: inhibition of prostate stromal cell growth and effects on smooth muscle contraction in the human prostate. *PloS one*, *11*(4), e0153312.

Wegner, A. M., Nebhan, C. A., Hu, L., Majumdar, D., Meier, K. M., Weaver, A. M., & Webb, D. J. (2008). N-wasp and the arp2/3 complex are critical regulators of actin in the development of dendritic spines and synapses. *Journal of Biological Chemistry*, *283*(23), 15912-15920.

Wu, S., Bellve, K. D., Fogarty, K. E., & Melikian, H. E. (2015). Ack1 is a dopamine transporter endocytic brake that rescues a trafficking-dysregulated ADHD coding variant. *Proceedings of the National Academy of Sciences*, *112*(50), 15480-15485.

Wu, W. J., Tu, S., & Cerione, R. A. (2003). Activated Cdc42 sequesters c-Cbl and prevents EGF receptor degradation. *Cell*, *114*(6), 715-725.

Yabroff, K. R., Lund, J., Kepka, D., & Mariotto, A. (2011). Economic burden of cancer in the United States: estimates, projections, and future research. *Cancer Epidemiology and Prevention Biomarkers*, *20*(10), 2006-2014.

Yang, N., Higuchi, O., Ohashi, K., Nagata, K., Wada, A., Kangawa, K., Nishida, E. & Mizuno, K.(1998). Cofilin phosphorylation by LIM-kinase 1 and its role in Rac-mediated actin reorganization. *nature*, *393*(6687), 809-812.

Ye, H., Zhang, Y., Geng, L., & Li, Z. (2015). Cdc42 expression in cervical cancer and its effects on cervical tumor invasion and migration. *International journal of oncology*, *46*(2), 757-763.

Yokoyama, N., Lougheed, J., & Miller, W. T. (2005). Phosphorylation of WASP by the Cdc42-associated Kinase ACK1 DUAL HYDROXYAMINO ACID SPECIFICITY IN A TYROSINE KINASE. *Journal of Biological Chemistry*, *280*(51), 42219-42226.

Zhang, X., Shang, X., Guo, F., Murphy, K., Kirby, M., Kelly, P., Reeves, L., Smith, F. O., Williams, D. A., Zheng, Y. & Pang, Q. (2008). Defective homing is associated with altered Cdc42 activity in cells from patients with Fanconi anemia group A. *Blood*, *112*(5), 1683-1686.

Zhao, L., Ma, Q. L., Calon, F., Harris-White, M. E., Yang, F., Lim, G. P., Morihara, T., Ubeda, O. J., Ambegaokar, S., Hansen, J. E., Weisbart, R. H., Teter, B., Frautschy, S. A. & Cole, G. M. (2006). Role of p21-activated kinase pathway defects in the cognitive deficits of Alzheimer disease. *Nature neuroscience*, *9*(2), 234-242.

Zheng, Y., Fischer, D. J., Santos, M. F., Tigyi, G., Pasteris, N. G., Gorski, J. L., & Xu, Y. (1996). The faciogenital dysplasia gene product FGD1 functions as a Cdc42Hs-specific guanine-nucleotide exchange factor. *Journal of Biological Chemistry*, *271*(52), 33169-33172.

Appendix A: Abbreviations

ACK-1: activated Cdc42 kinase 1
AID: autoinhibitory domain
ALS: amyotrophic lateral sclerosis
ANOVA: analysis of variance
AR: androgen receptor
Arp2/3: actin related protein 2/3
BD: basic domain
BSA: bovine serum albumin
Cdc42: cell division control protein 42
CGN: cerebellar granule neuron
CML: chronic myelogenous leukemia
CRIB: Cdc42/Rac interactive binding motif
Cy3: indocarbocyanine
Dbl: diffuse B-cell lymphoma
DH: Dbl homology
DMSO: dimethyl sulfoxide
DOCK: dedicator of cytokinesis
DRG: dorsal root ganglion
EBD: EGFR binding domain
EGFR: epidermal growth factor receptor
FBS: fetal bovine serum
FITC: fluorescein isothiocyanate
FKHR: forkhead box protein
G-LISA: GTPase-linked immunosorbent assay
GAP: GTPase activating protein
GBD: GTPase binding domain
GBM: glioblastoma multiforme
GDI: guanine nucleotide dissociation inhibitor
GDP: guanosine diphosphate
GEF: guanine nucleotide exchange factor
GFP: green fluorescence protein
GPCR: G-protein coupled receptor
GTP: guanosine triphosphatase
IAPs: inhibitor of apoptosis proteins
HRP: horseradish peroxidase
JAK/STAT: janus kinase/signal transducers and activators of transcription
LIMK: LIM kinase
LPA: lysophosphatidic acid
mAChR: muscarinic cholinergic receptor
MAPK: mitogen activated protein kinase
MEFs: mouse embryonic fibroblasts
MLC: myosin II regulatory light chain

MLCK: myosin light chain kinase
MOI: multiplicity of infection
MRX: mental X-linked retardation
N-WASp: neuronal Wiskott-Aldrich syndrome protein
NMR: nuclear magnetic resonance
PAK: p21-activated kinase
PBS: phosphate buffered saline
PBS-T: phosphate buffered saline + Tween 20
PFM: paraformaldehyde
PH: Pleckstrin homology
PI3K: phosphoinositide-3-kinase
PIP_2: phosphatidylinositol 4,5-bisphosphate
PIP_3: phosphatidylinositol (3,4,5)-trisphosphate
PVDF: polyvinylidene difluoride
RISC: RNA induced silencing complex
RNAi: RNA interference
ROCK/PTEN: Rho-associated protein kinase/phosphatase and tensin homolog
SAM: sterile alpha motif
SEM: standard Error of the Mean
shRNA: short-hairpin RNA
UBA: ubiquitination
VCA: verprolin homology, cofilin homology, acidic
WAS: Wiskott-Aldrich syndrome
WASp: Wiskott-Aldrich syndrome protein
WH1: WASp-homology 1
WIP: WASp interacting protein
WWox: WW domain-containing oxioreductase